AD_______________

Award Number: W81XWH-12-1-0356

TITLE: A Specific Screening Strategy to Reduce Prostate Cancer Mortality

PRINCIPAL INVESTIGATOR: Kurt R. Zinn

CONTRACTING ORGANIZATION: University of Alabama at Birmingham
Birmingham, AL 35294

REPORT DATE: September 2013

TYPE OF REPORT: Annual

PREPARED FOR: U.S. Army Medical Research and Materiel Command
Fort Detrick, Maryland 21702-5012

REPORT DOCUMENTATION PAGE

Form Approved
OMB No. 0704-0188

1. REPORT DATE
September 2013

2. REPORT TYPE
Annual

3. DATES COVERED
15 August 2012 -14 August 2013

4. TITLE AND SUBTITLE
A Specific Screening Strategy to Reduce Prostate Cancer Mortality

5a. CONTRACT NUMBER

5b. GRANT NUMBER
W81XWH-12-1-0356

5c. PROGRAM ELEMENT NUMBER

6. AUTHOR(S)
Kurt R. Zinn

E-Mail: kurtzinn@uab.edu

5d. PROJECT NUMBER

5e. TASK NUMBER

5f. WORK UNIT NUMBER

7. PERFORMING ORGANIZATION NAME(S) AND ADDRESS(ES)

University of Alabama at Birmingham
Birmingham, AL 35294

8. PERFORMING ORGANIZATION REPORT NUMBER

9. SPONSORING / MONITORING AGENCY NAME(S) AND ADDRESS(ES)
U.S. Army Medical Research and Materiel Command
Fort Detrick, Maryland 21702-5012

10. SPONSOR/MONITOR'S ACRONYM(S)

11. SPONSOR/MONITOR'S REPORT NUMBER(S)

12. DISTRIBUTION / AVAILABILITY STATEMENT
Approved for Public Release; Distribution Unlimited

13. SUPPLEMENTARY NOTES

14. ABSTRACT
We report the use of a cancer-specific promoter, inhibition of differentiation (Id1), to drive a dual-reporter diagnostic system (Ad5/3-Id1-SEAP-Id1-mCherry) for sensitive detection of prostate cancer using a blood-based reporter SEAP (secreted embryonic alkaline phosphatase) and tumor localization using a fluorescent reporter protein, mCherry. To evaluate the performance of this system, a prostate cell panel (WPMY-1, LNCaP, Du145, MDA-PCA-2b, VCaP, and PC3) of varying degrees of malignancy and aggressiveness was tested. Id1 expression of the prostate cell panel was measured by Western blot. Following infection with the Ad5/3-Id1-SEAP-Id1-mCherry vector, expression of the SEAP and mCherry reporters was determined. PSA levels were also measured for each cell type. Although no correlation was observed between Id1 levels and PSA (R^2=0.01), SEAP reporter expression was found to significantly correlate (R^2=0.89) with Id1 and cancer cell aggressiveness. The fluorescent mCherry reporter protein was used for *in vivo* localization of prostate cancer cells following flank implantation. Both non-aggressive LNCaP and aggressive PC3 prostate cancer cells were visualized 2 days post-implantation with a fluorescence intensity that corresponded to cancer aggressiveness and total tumor cell infectivity. These data support the use of the Ad5/3-Id1-SEAP-Id1-mCherry diagnostic vector as a predictor of prostate cancer malignancy and a strategy for non-invasive tumor localization.

15. SUBJECT TERMS
prostate cancer screening, imaging, ID1

16. SECURITY CLASSIFICATION OF:			**17. LIMITATION OF ABSTRACT**	**18. NUMBER OF PAGES**	**19a. NAME OF RESPONSIBLE PERSON** USAMRMC
a. REPORT U	**b. ABSTRACT** U	**c. THIS PAGE** U	UU	51	**19b. TELEPHONE NUMBER** *(include area code)*

Table of Contents

Introduction:

The goal of the proposed research is early detection of relevant prostate cancer to reduce mortality of the disease. This will be accomplished by introduction of an improved and more specific diagnostic procedure. According to the American Cancer Society, prostate cancer is the second leading cause of cancer-related deaths in men. It is estimated that 1 man in every 36 will die of prostate cancer during their lifetime. This accounts for 33,720 men in 2011. Early and accurate detection of prostate cancer is an urgent priority. Our research strategy will introduce a new paradigm in prostate cancer detection, moving beyond prostate-specific antigen (PSA) screening into an advanced and specific strategy to improve detection and resection, and thereby reduce prostate cancer mortality.

We hypothesize that an effective strategy for the detection of prostate cancer will use Id1 to direct a combined blood-based monitoring and imaging system following systemic delivery and controlled release in the prostate vasculature. This diagnostic system includes a secreted human embryonic alkaline phosphatase reporter for blood-based monitoring and a mCherry reporter for localized imaging, both under the control of an Id1 promoter, and packaged in an Adenovirus for ease in testing. Id1 expression has been shown to be specific for malignant cancers and will permit differentiation between aggressive cancer and benign hyperplasia. To permit non-invasive and effective systemic delivery of the diagnostic Ad, US contrast agents, or MBs, will be used to deliver the diagnostic vector to the tumor in an US-targeted strategy. Our hypothesis will be tested using the following specific aims:

1. Correlate prostate cancer phenotype with SEAP/mCherry levels achieved with the diagnostic vector (Ad5/3-Id1-SEAP-Id1-mCherry), an existing vector encoding SEAP and mCherry.
2. Optimize and validate Ad5/3-Id1-SEAP-Id1-mCherry loading of ultrasound (US) microbubbles (MBs).
3. Determine the efficacy of the diagnostic vector combined with the US delivery system to detect malignant prostate cancer.

Our proposed diagnostic system addresses a **PCRP Overarching Challenge** by developing a clinically feasible way to distinguish between aggressive and indolent cancers. Our proposed system is a huge improvement on PSA testing. The goal of our proposal is to generate a cancer-specific approach to prostate cancer screening and improved surgical resection. At the foundation of the diagnostic strategy proposed here is a cancer-specific promoter whose level of expression specifically correlates with the aggressive phenotype of the cancer. This allows the diagnostic vector to be a tool for detection and an indicator of malignancy. In addition to the Overarching Challenge, this proposal also addresses the prostate cancer imaging **Focus Area**.

Body: The accomplishments associated with the three specific aims are summarized below. All of the accomplishments have been included in manuscripts, either submitted or approaching submission. The manuscripts are included as appendices and provide all details of the methods used.

Task 1. **Specific Aim #1: Correlate prostate cancer phenotype with SEAP/mCherry levels achieved with the diagnostic vector (Ad5/3-Id1-SEAP-Id1-mCherry), an existing vector encoding SEAP and mCherry.** ***(Primarily first year, except aim1d that may run in to 2nd year)***

a. Ad3 receptor expression characterization: A prostate cancer cell panel (PC3, LNCaP, CA-HPV-10, RWPE-1, VCAP, MDA PCA 2b, WPMY-1, DU145) will be analyzed for Ad3 receptor expression. ***(Months 1-4)***

Accomplishment: Ad3 receptor surface expression was quantified for each cell type in the panel by infection with an Ad5/3-CMV-Luc adenovirus. Luciferase counts were subsequently used to normalize diagnostic reporter expression, accounting for differences in Ad5/3-Id1-SEAP-Id1-mCherry infectivity among the cells. SEAP and mCherry reporter expressions were therefore only a reflection of Id1 promoter activity. Results are reported under task 1c, together with results for ID1 expression.

b. The panel of cell lines will be characterized for Id1 promoter expression. ***(Months 1-6)***

Accomplishment: Id1 expression, but not PSA level, is an indicator of prostate cancer cell aggressiveness. Six prostate cell lines purchased from ATCC were categorized based on their reported behaviors and measured levels of PSA secretion (Table 1). Normal prostate cells (WPMY-1) secreted a baseline amount of 314.1±8.1 pg/mL PSA. Two of the four cell lines with reportedly aggressive phenotypes (Du145 and PC3) had relatively lower PSA levels, ranging from 230-266 pg/mL, whereas the remaining aggressive cells lines (VCaP and MDA-PCA-2b) had significantly greater levels of PSA as compared to baseline. The one non-aggressive cell type, LNCaP, also secreted significantly increased amounts of PSA in comparison to baseline levels. Id1 expression was elevated in all prostate cancer cell types with reportedly aggressive behaviors compared to normal prostate cells and cancerous cells with a less invasive and non-aggressive phenotype (Figure 1a). No correlation was found between Id1 expression and PSA level (R^2=0.058; Figure 1b).

Table 1. Description of cell lines used for analyses of Ad5/3-Id1-SEAP-Id1-mCherry diagnostic efficacy.

Cell Line	Origin	Behavior	PSA (pg/mL)
WPMY-1	Normal stromal myofibroblast	Normal	324.6±21.5
Du145	Brain metastasis	Aggressive	230.1±8.3**
PC3	Bone metastasis	Aggressive	266.2±36.7*
VCaP	Vertebral metastasis	Aggressive	762.9±36.4**
MDA-PCA-2b	Bone metastasis	Aggressive	11,227±1274**
LNCaP	Node metastasis	Non-Aggressive	13,042±315**

PSA values reported as mean±SEM (n=3). *p<0.05 and **p<0.001 versus WPMY-1 level.

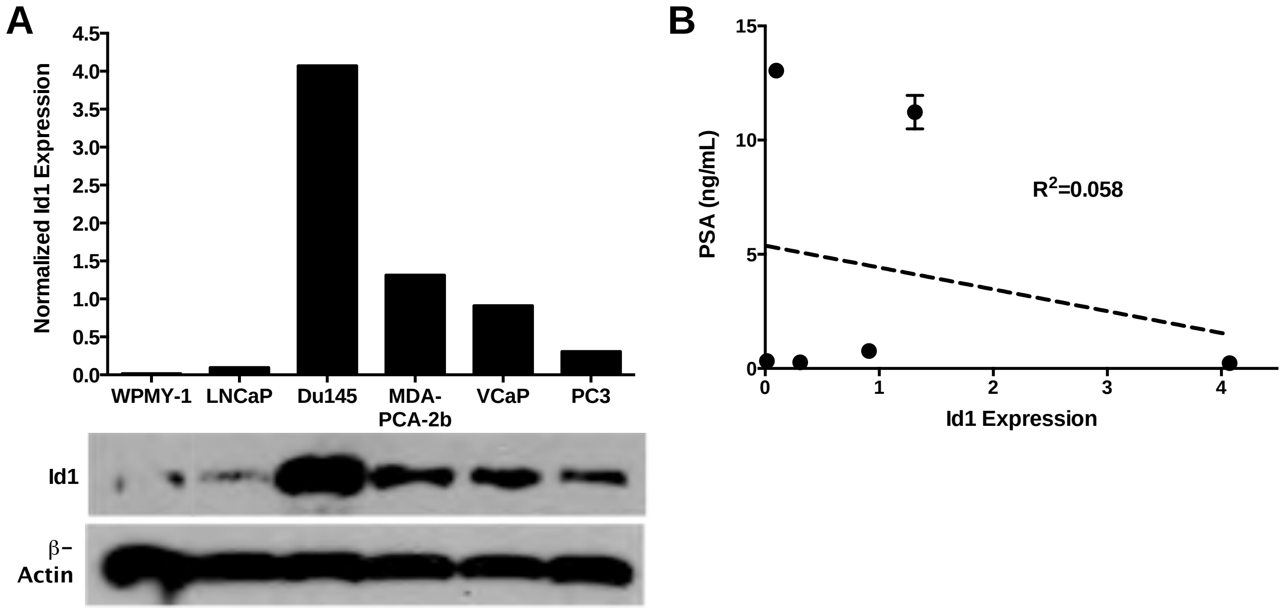

Figure 1. Cellular expression of Id1 does not correlate with PSA. (a) Id1 expression was evaluated in cell lysates by Western blot and quanitified with densitometry. Id1 intensity was normalized to the corresponding level of of β-actin. **(b)** Linear regression analysis was used to correlate cellular Id1 expression with PSA levels reported in Table 1. PSA data are shown as mean±SEM (n=3).

c. **Diagnostic vector infection of prostate cancer panel: The performance of the diagnostic vector with the cell panel will be evaluated. Reporter values will be normalized against Ad3 receptor expression. Id1 knockdown experiments will be conducted.** ***(Months 6-12)***

Accomplishment: SEAP and mCherry reporter expression correlate with Id1 levels and are indicators of prostate cell aggressiveness As stated under 1a, Ad3 receptor surface expression was quantified for each cell type in the panel by infection with an Ad5/3-CMV-Luc adenovirus (Figure 2a). Luciferase counts were subsequently used to normalize diagnostic reporter expression, accounting for differences in Ad5/3-Id1-SEAP-Id1-mCherry infectivity among the cells. SEAP and mCherry reporter expressions were therefore only a reflection of Id1 promoter activity. After infection with Ad5/3-Id1-SEAP-Id1-mCherry, the prostate cancer lines with aggressive phenotypes (VCaP, MDA-PCA-2b, PC3, and Du145) had increased levels of SEAP reporter compared to non-aggressive (LNCaP) and normal (WPMY-1) cells (Figure 2b). For PC3 and Du145, Ad3-normalized SEAP expression was significantly elevated at 4 and 6 days post-infection compared to non-aggressive LNCaP cells at the corresponding timepoints. A significant correlation (R^2=0.89) between SEAP reporter expression at day 4 and cellular Id1 levels was observed (Figure 2c). Likewise, representative fluorescent images of the mCherry reporter qualitatively confirmed diagnostic vector efficiency (Figure 3). mCherry intensity corresponded to cellular Id1 levels, with the greatest fluorescence observed in the aggressive Du145 cells.

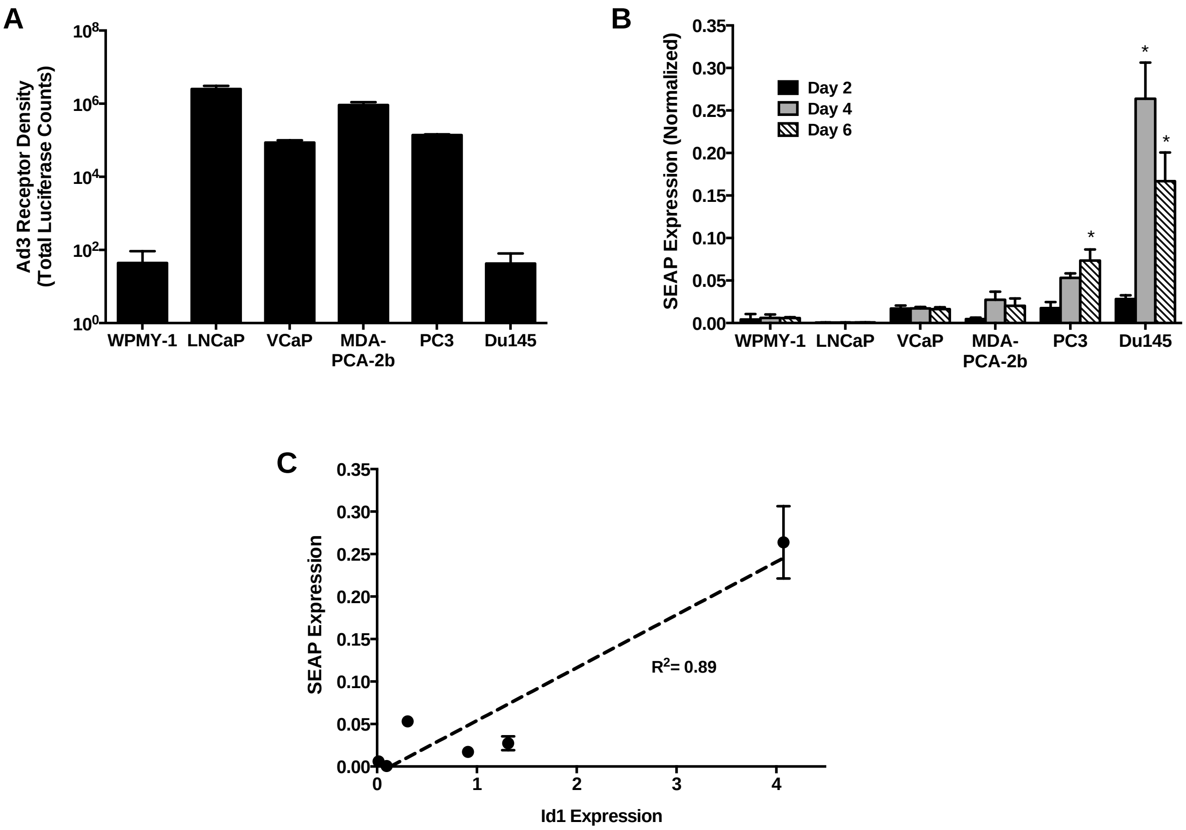

Figure 2. SEAP reporter expression increases with aggressiveness of prostate cancer cell and correlates with cellular level of Id1. (a) Ad3 receptor density for each cell type was determined following infection with an Ad5/3-CMV-Luc adenovirus (MOI=10). **(b)** SEAP reporter was measured in culture medium 2, 4 and 6 days post-infection with Ad5/3-Id1-SEAP-Id1-mCherry (MOI=1) and normalized with Ad3 receptor surface expression. *$p<0.01$ versus LNCap at corresponding timepoint. **(b)** Linear regression analysis was used to correlate SEAP reporter expression and cellular Id1. All data are reported as mean±SEM (n=4).

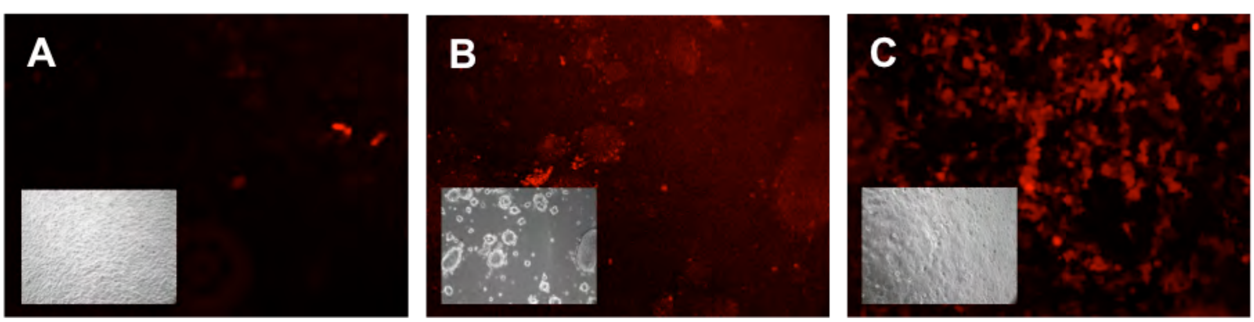

Figure 3. mCherry reporter fluorescence corresponds to prostate cancer cell aggressiveness. Representative fluorescence images of **(a)** normal prostate cells (WPMY-1) and cancerous cells with **(b)** moderate Id1 expression (VCaP) and **(c)** high Id1 expression (Du145). Inserts are corresponding bright field images. All images were acquired using a 10X objective.

d. Assessment of the diagnostic potential of the vector on normal, BPH, and malignant tissue samples of the prostate: In addition to reporter expression characterization, Id1 and Ad3 expression will be evaluated and normalized against reporter values. (n=10/group)*(Months 1-18)*

Accomplishment. The use of human tissue samples was a lower priority objective until the diagnostic vector was produced and evaluated. Our findings will be reported in the 2nd year progress report.

Task 2. Specific Aim #2: Optimize and validate Ad5/3-Id1-SEAP-Id1-mCherry loading of ultrasound microbubbles. ***(Start month 9, ending at month 18 (middle of year 2))***

a. Qualitative visualization of Ad packaged microbubbles: Using fluorescent confocal microscopy, microbubble packaged, fluorescent Ad particles containment will be analyzed. *(Months 9-12)*

Accomplishment. We decided that before packaging experiments it was important to understand if the ultrasonograpy would change Ad infectivity due to disruption of the Ad particles. We also sought to understand if microbubbles with ultrasound would aid in allowing the Ad particle to better infect prostate cancer cells. The results of these studies are summarized below in the abstract of an in-press manuscript entitled "Enhancement of Adenovirus Delivery after Ultrasound-Stimulated Therapy in a Cancer Model".

Improving the efficiency of adenovirus (Ad) delivery to target tissues has the potential to advance the translation of cancer gene therapy. Ultrasound (US)-stimulated therapy utilizes microbubbles (MBs) exposed to low-intensity US energy to improve localized delivery. We hypothesize that US-stimulated gene therapy can improve Ad infection in a primary prostate tumor through enhanced tumor uptake and retention of the Ad vector. *In vitro* studies were performed to analyze the degree of Ad infectivity after application of US-stimulated gene therapy. A luciferase-based Ad on a ubiquitous cytomegalovirus (CMV) promoter (Ad5/3-CMV-Luc) was used in an animal model of prostate cancer (bilateral tumor growth) to evaluate Ad transduction efficiency after US-stimulated therapy. Bioluminescence imaging was employed for *in vivo* analysis to quantify Ad infection within the tumor. *In vitro* studies revealed no difference in Ad transduction between groups receiving US-stimulated therapy using high, low, or sham US intensity exposures at various multiplicity of infections (MOIs) ($p = 0.80$). *In vivo* results showed that tumors receiving US-stimulated therapy after intratumoral injection of Ad5/3-CMV-Luc (1×10^6 plaque forming units) demonstrated a 95.1% enhancement in tumor delivery compared to control tumors receiving sham US ($p = 0.03$). US-stimulated therapy has significant potential to immediately impact Ad-based cancer gene therapy by improving virus bioavailability in target tissues.

The other task 2 objectives were for year 2 of the funding period.

Task 3: Specific Aim #3: Determine the efficacy of the diagnostic vector combined with the US delivery system to detect malignant prostate cancer. ***(Start month 18 and continue to month 36)***

a. In vivo analysis of diagnostic vector in xenograft animal model (30 athymic nude mice) to determine detection sensitivity. *(Months 18-24)*

Accomplishment. Although aim #3 objectives were for later time periods, we decided to move forward with initial animal experiments, and report our progress.

Fluorescent mCherry reporter allows for *in vivo* localization of aggressive and non-aggressive tumors. Two days after flank implantation of Ad5/3-Id1-SEAP-Id1-mCherry-infected PC3 and LNCaP cells, the mCherry reporter protein was fluorescently detected. Representative images of mCherry expression illustrate that aggressive PC3 cells were visually detected at both low (Figure 4a) and high (Figure 4b) levels of total cell infectivity (2.5% and 17.5% of total tumor cells, respectively). Non-aggressive LNCaP cells were also detected at higher levels of infectivity (Figure 4d), however, mCherry fluorescence was not observable when only 2.5% of the total cells were infected (Figure 4c). Quantification of mCherry fluorescence with ROI analyses confirmed that reporter intensity corresponded to cancer cell aggressiveness and total infectivity since the most significant fluorescence was observed with the aggressive PC3 cells at 17.5% total infectivity (Figure 4e).

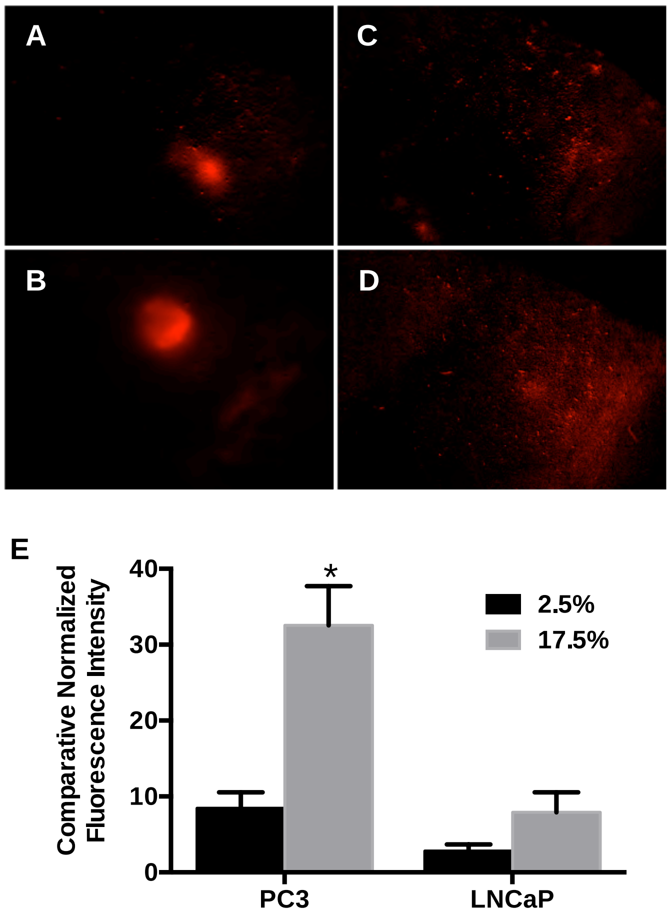

Figure 4. Infected tumors are visualized *in vivo* with the fluorescent mCherry reporter. (a-d) Representative images of mCherry reporter expression 2 days after flank implantation of PC3 **(a,b)** and LNCaP **(c,d)** cells with 2.5% **(a,c)** and 17.5% **(b,d)** total cell infectivity. PC3 and LNCaP cells were infected with Ad5/3-Id1-SEAP-Id1-mCherry for 24h and then implanted with non-infected cells to simulate low (2.5%) or high (17.5%) tumor infectivity. **(e)** Quantitative region of interest analysis of tumor fluorescence was done to measure mCherry reporter intensity following implantation. All data are reported as mean±SEM (n=4). *p<0.001 versus all groups.

The other task 3 objectives were scheduled for year 2-3 of the funding period.

Key Research Accomplishments:

- We evaluated ID1 expression in a panel of prostate cancer cell lines.

- We identified differences in Ad infectivity of prostate cancer cell lines, which could be used to normalize the cell lines for comparisons.

- Unlike measurements of PSA, which showed no correlation with cellular Id1, expression of the blood-based SEAP reporter showed a significant correlation with prostate cancer cell aggressiveness.

- We demonstrated that ultrasound did not change Ad infectivity.

- We demonstrated that ultrasound with microbubbles improved Ad infectivity in a prostate cancer model.

Reportable Outcomes:

Manuscript in press:

1. Sorace AG, Warram JM, Mahoney M, Zinn KR, **Hoyt K**. Enhancement of adenovirus delivery after ultrasound-stimulated therapy in a cancer model. Ultrasound in Medicine and Biology, 2013

Manuscript in preparation:

1. Richter JR, Mahoney M, Warram JM, Samuel S, Zinn KR. A Dual-reporter, Diagnostic Vector For Detection and Localization of Prostate Cancer. *Mol Ther.*

Abstracts Published:

1. Sorace AG, Mahoney M, Zinn KR, **Hoyt K**. Volumetric molecular ultrasound imaging of tumor vascularity in a preclinical model of prostate cancer. American Institute for Ultrasound in Medicine Annual Convention, 32:S16, 2013.

Abstracts accepted and presentations scheduled:

1. Warram JM, Mahoney M, Zinn KR. "Combined imaging and screening of prostate cancer." *2013 World Molecular Imaging Congress.* Savannah, Georgia. 2013.
2. Sorace AG, Warram JM, Mahoney M, Zinn KR, Hoyt K. Ultrasound-stimulated gene therapy for improved adenovirus infection. World Molecular Imaging Congress, 2013
3. Warram JM, Sorace AG, Mahoney M, Samuel S, Harbin B, Joshi M, Martin A, Whitworth L, Hoyt K, Zinn KR. Biodistribution of P-selectin targeted microbubbles. World Molecular Imaging Congress, 2013.
4. Richter JR, Mahoney M, Warram JM, Samuel S, Zinn KR. "A dual-reporter, diagnostic vector for detection and localization of prostate cancer." *2013 UAB Comprehensive Cancer Center Retreat.* Birmingham, Alabama. 2013.

Invited for presentation

1. Hoyt K. Molecular ultrasound imaging. American Institute for Ultrasound in Medicine Annual Convention, 2014 (**Invited** for presentation).

Degree Awarded

M.S. degree to Marshall Mahoney

Employment or research opportunities applied for and/or received based on experience/training supported by this award.

Dr. Jason Warram was hired as an Instructor in the UAB Department of Surgery, effective Oct. 1, 2013

Conclusions

In the first year, a dual reporter vector, Ad5/3-Id1-SEAP-Id1-mCherry, was evaluated for its ability to noninvasively detect and monitor prostate cancer using expression of a SEAP reporter for blood-based detection and mCherry reporter for fluorescence imaging. Reporter expression of the diagnostic system was driven by the cancer-specific expression of Id1, which is a documented indicator of tumor malignancy with no expression found in BPH and normal prostate. The present study used a panel of prostate cancer cells with varying degrees of reported aggressiveness in addition to normal prostate cells. Measurement of cellular levels of Id1 was used to quantify aggressiveness, allowing us to assess the relationship between cancer malignancy and diagnostic efficacy of the Ad5/3-Id1-SEAP-Id1-mCherry vector. Unlike measurements of PSA, which showed no correlation with cellular Id1, expression of the blood-based SEAP reporter showed a significant correlation with cancer cell aggressiveness.

Implantation of infected, tumor-forming cells demonstrated that the Ad5/3-Id1-SEAP-Id1-mCherry diagnostic vector can be used for *in situ* detection and localization of prostate cancer. By simulating low (2.5%) and high (17.5%) tumor cell infectivity, we demonstrated sensitive visualization of tumors formed by both aggressive (PC3) and non-aggressive (LNCaP) prostate cancer cells. Fluorescent mCherry reporter expression was detected in aggressive tumors with both high and low infectivity and non-aggressive tumors with high infectivity. The lower limit of detection for tumor visualization using mCherry fluorescence, however, was approached with poorly infected, non-aggressive LNCaP tumors. Since reporter expression is dependent on cellular Id1 expression and LNCaP cells have relatively low levels of Id1, greater tumor infectivity is needed for accurate localization.

The dependency of the diagnostic vector on adequate expression of Id1 represents a limitation of the current system for detecting less aggressive cancers. However, by achieving targeted delivery and increased tumor infectivity, the visual detection limits of the diagnostic vector can be surpassed. Our future work will aim to develop strategies to target vector delivery and infectivity of both aggressive and non-aggressive prostate cancer to allow for sensitive localization to aid in tumor resection.

In conclusion, the present work introduces a novel strategy for detection and localization of prostate cancer that overcomes the current limitations of the PSA test to distinguish between aggressive cancer and indolent conditions like BPH. The correlation between reporter expression and cellular Id1 enables SEAP levels to be used as a predictive measure of prostate cancer aggressiveness and mCherry fluorescence as an aid for tumor visualization. This strategy would assist clinicians in the detection and treatment of prostate cancer and ultimately reduce the mortality associated with this disease.

Personnel supported by this grant:

Dr. Kurt R. Zinn, PI
Dr. Kenneth Hoyt
Dr. Jason Warram (post-doctoral fellow, taking faculty position at UAB in Oct. 2013)
Dr. Jill Richter (post-doctoral fellow, recruited to take Dr. Warram's position on the grant)
Dr. Sudarshan
Marshall Mahoney (M.S. student, graduated in May 2013 with M.S. degree)
Sharon Samuel

A Dual-Reporter, Diagnostic Vector for Detection and Localization of Prostate Cancer

Jillian R. Richter[1], Marshall Mahoney[2], Jason M. Warram[3], Sharon Samuel[1], Kurt R. Zinn[1]

[1]Department of Radiology, University of Alabama at Birmingham, Birmingham, AL 35294,
[2]Department of Biomedical Engineering, University of Alabama at Birmingham, Birmingham, AL 35294
[3]Department of Pathology, University of Alabama at Birmingham, Birmingham, AL 35294

Running Title: Diagnostic Vector for Prostate Cancer Detection

Keywords: adenovirus, inhibitor of differentiation (Id1), PSA, mCherry, SEAP, imaging, detection

Funding Source: This work was supported the UAB Small Animal Imaging Shared Facility NIH Research Core Grant (P30CA013148) and the DOD Prostate Cancer Research Program (PC111230).

Conflict of Interest: None

ABSTRACT

Detection of prostate-specific antigen (PSA) as a screening strategy for prostate cancer is limited by the inability of the PSA test to differentiate between malignant cancer and benign hyperplasia. Here, we report the use of a cancer-specific promoter, inhibition of differentiation (Id1), to drive a dual-reporter diagnostic system (Ad5/3-Id1-SEAP-Id1-mCherry) for sensitive detection of prostate cancer using a blood-based reporter SEAP (secreted embryonic alkaline phosphatase) and tumor localization using a fluorescent reporter protein, mCherry. To evaluate the performance of this system, a prostate cell panel (WPMY-1, LNCaP, Du145, MDA-PCA-2b, VCaP, and PC3) of varying degrees of malignancy and aggressiveness was tested. Id1 expression of the prostate cell panel was measured by Western blot. Following infection with the Ad5/3-Id1-SEAP-Id1-mCherry vector, expression of the SEAP and mCherry reporters was determined. PSA levels were also measured for each cell type. Although no correlation was observed between Id1 levels and PSA (R^2=0.01), SEAP reporter expression was found to significantly correlate (R^2=0.89) with Id1 and cancer cell aggressiveness. The fluorescent mCherry reporter protein was used for *in vivo* localization of prostate cancer cells following flank implantation. Both non-aggressive LNCaP and aggressive PC3 prostate cancer cells were visualized 2 days post-implantation with a fluorescence intensity that corresponded to cancer aggressiveness and total tumor cell infectivity. These data support the use of the Ad5/3-Id1-SEAP-Id1-mCherry diagnostic vector as a predictor of prostate cancer malignancy and a strategy for non-invasive tumor localization.

INTRODUCTION

According to the American Cancer Society, prostate cancer is the second leading cause of cancer-related deaths in men. It is estimated that 1 man in every 36 will die of prostate cancer accounting for 33,720 men in 2011 [1]. With an aging baby-boomer population, the prevalence of prostate cancer is estimated to increase to 450,000 diagnoses in 2015 [2]. Therefore, early and accurate detection of prostate cancer is an urgent priority.

Since 1986, screening for prostate cancer has relied heavily on the detection of prostate specific antigen (PSA) in the blood. The relative levels of PSA predict the abnormal presence of hyperplasia in the prostate. However, the PSA test cannot distinguish between lethal and non-lethal disease due to the low specificity of the test to differentiate aggressive cancer [3-7]. Considering these limitations, an improved method for prostate cancer screening is needed to accurately distinguish between aggressive and indolent cancers.

Inhibitor of Differentiation (Id1) is a member of the inhibitor of differentiation family of transcription factors. They form inactive heterodimers with basic helix-loop-helix (bHLH) family of transcription factors that control cellular processes such as cell-fate determination, proliferation, cell-cycle regulation, angiogenesis, invasion, and migration [8, 9]. Id1 gene expression is cancer-specific and has been demonstrated to have increasing levels in human tumors that correlate with increasing Gleason grade and progression [10]. Several studies [11-15] have shown expression of Id1 to be an indicator of malignancy with no expression found in cases of benign prostate hyperplasia (BPH) and normal prostate tissue. The correlation between increased Id1 expression and cancer aggressiveness supports the use of the Id1 promoter for controlling diagnostic reporter function.

Secreted embryonic alkaline phosphatase (SEAP) is a truncated and secreted form of human embryonic alkaline phosphatase that is extremely stable and nonimmunogenic. Due to its heat stability and resistance to the phosphatase inhibitor L-homoarginine, SEAP levels can be measured independently from endogenous alkaline phosphatase activity with high sensitivity. The imaging reporter, mCherry, has an excitation peak of 587 nm and emission peak of 610 nm, and is a mutated variant of the widely used mRFP1. The mCherry protein matures more quickly and completely than mRFP1, yielding higher extinction coefficient and brightness, yet bleaches 10-times more slowly [16]. The longer wavelength of mCherry decreases the interference from tissue auto-fluorescence and allows for greater tissue penetration. Finally, mCherry can be detected by fluorescence imaging in the surgical setting using laparoscopic techniques, including robotic surgery (e.g. daVinchi), to improve surgical treatment of relevant prostate cancer.

Recently, the diagnostic vector, Ad5/3-Id1-SEAP-Id1-mCherry, was constructed and shown to be highly specific and sensitive for breast cancer detection in both in vitro and in vivo models [17]. With this vector, dual-reporter expression of secreted embryonic alkaline phosphatase (SEAP) and the fluorescent protein mCherry is driven by the cancer-specific promoter inhibitor of differentiation (Id1) and allows for both blood-based screening and localized visualization of cancer. Importantly, since both reporters are under the control of Id1, specific for aggressive cancer phenotypes, reporter expression is a relative indicator of prognosis.

In the present study, we evaluate the use of Ad5/3-Id1-SEAP-Id1-mCherry as a diagnostic system for screening prostate cancer using normal cells and cancer cell lines of various aggressive phenotypes. By correlating Id1 expression with SEAP levels and mCherry fluorescence, we assess the effectiveness of Ad5/3-Id1-SEAP-Id1-mCherry in predicting cancer cell phenotype in comparison to the PSA test. In addition, we determine the applicability of using the diagnostic vector for *in vivo* detection and localization. The dual-reporter vector represents a novel method for non-invasively measuring cancer aggressiveness and visually monitoring prostate cancer, ultimately overcoming the limitations associated with PSA test-based diagnoses and, thus, leading to improved treatment efficacy.

RESULTS

Id1 expression, but not PSA level, is an indicator of prostate cancer cell aggressiveness

Six prostate cell lines purchased from ATCC were categorized based on their reported behaviors [18-23] and measured levels of PSA secretion (Table 1). Normal prostate cells (WPMY-1) secreted a baseline amount of 314.1±8.1 pg/mL PSA. Two of the four cell lines with reportedly aggressive phenotypes (Du145 and PC3) had relatively lower PSA levels, ranging from 230-266 pg/mL, whereas the remaining aggressive cells lines (VCaP and MDA-PCA-2b) had significantly greater levels of PSA as compared to baseline. The one non-aggressive cell type, LNCaP, also secreted significantly increased amounts of PSA in comparison to baseline levels. Id1 expression was elevated in all prostate cancer cell types with reportedly aggressive behaviors compared to normal prostate cells and cancerous cells with a less invasive and non-aggressive phenotype (Figure 1a). No correlation was found between Id1 expression and PSA level (R^2=0.058; Figure 1b).

Table 1. Description of cell lines used for analyses of Ad5/3-Id1-SEAP-Id1-mCherry diagnostic efficacy.

Cell Line	Origin	Behavior	PSA (pg/mL)
WPMY-1	Normal stromal myofibroblast	Normal [18]	324.6±21.5
Du145	Brain metastasis	Aggressive [19]	230.1±8.3**
PC3	Bone metastasis	Aggressive [20]	266.2±36.7*
VCaP	Vertebral metastasis	Aggressive [21]	762.9±36.4**
MDA-PCA-2b	Bone metastasis	Aggressive [22]	11,227±1274**
LNCaP	Node metastasis	Non-Aggressive [23]	13,042±315**

PSA values reported as mean±SEM (n=3). *p<0.05 and **p<0.001 versus WPMY-1 level.

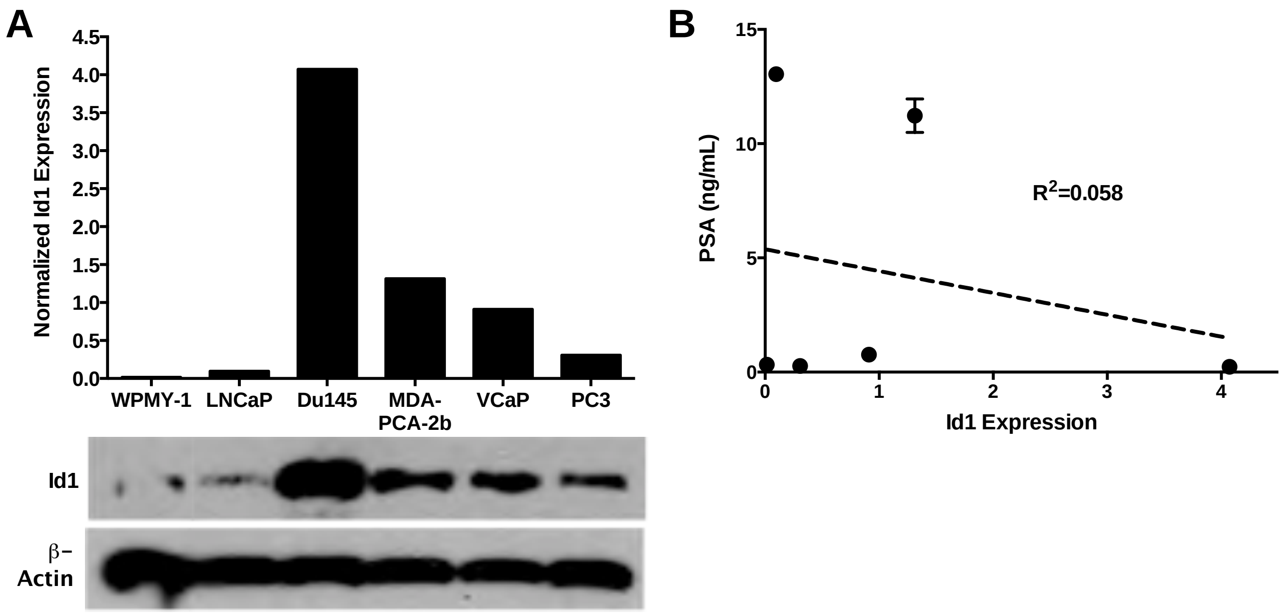

Figure 1. Cellular expression of Id1 does not correlate with PSA. (a) Id1 expression was evaluated in cell lysates by Western blot and quanitified with densitometry. Id1 intensity was normalized to the corresponding level of of β-actin. **(b)** Linear regression analysis was used to correlate cellular Id1 expression with PSA levels reported in Table 1. PSA data are shown as mean±SEM (n=3).

SEAP and mCherry reporter expression correlate with Id1 levels and are indicators of prostate cell aggressiveness

Ad3 receptor surface expression was quantified for each cell type in the panel by infection with an Ad5/3-CMV-Luc adenovirus (Figure 2a). Luciferase counts were subsequently used to normalize diagnostic reporter expression, accounting for differences in Ad5/3-Id1-SEAP-Id1-mCherry infectivity among the cells. SEAP and mCherry reporter expressions were therefore only a reflection of Id1 promoter activity. After infection with Ad5/3-Id1-SEAP-Id1-mCherry, the prostate cancer lines with aggressive phenotypes (VCaP, MDA-PCA-2b, PC3, and Du145) had increased levels of SEAP reporter compared to non-aggressive (LNCaP) and normal (WPMY-1) cells (Figure 2b). For PC3 and Du145, Ad3-normalized SEAP expression was significantly elevated at 4 and 6 days post-infection compared to non-aggressive LNCaP cells at the corresponding timepoints. A significant correlation (R^2=0.89) between SEAP reporter expression at day 4 and cellular Id1 levels was observed (Figure 2c). Likewise, representative fluorescent images of the mCherry reporter qualitatively confirmed diagnostic vector efficiency (Figure 3). mCherry intensity corresponded to cellular Id1 levels, with the greatest fluorescence observed in the aggressive Du145 cells.

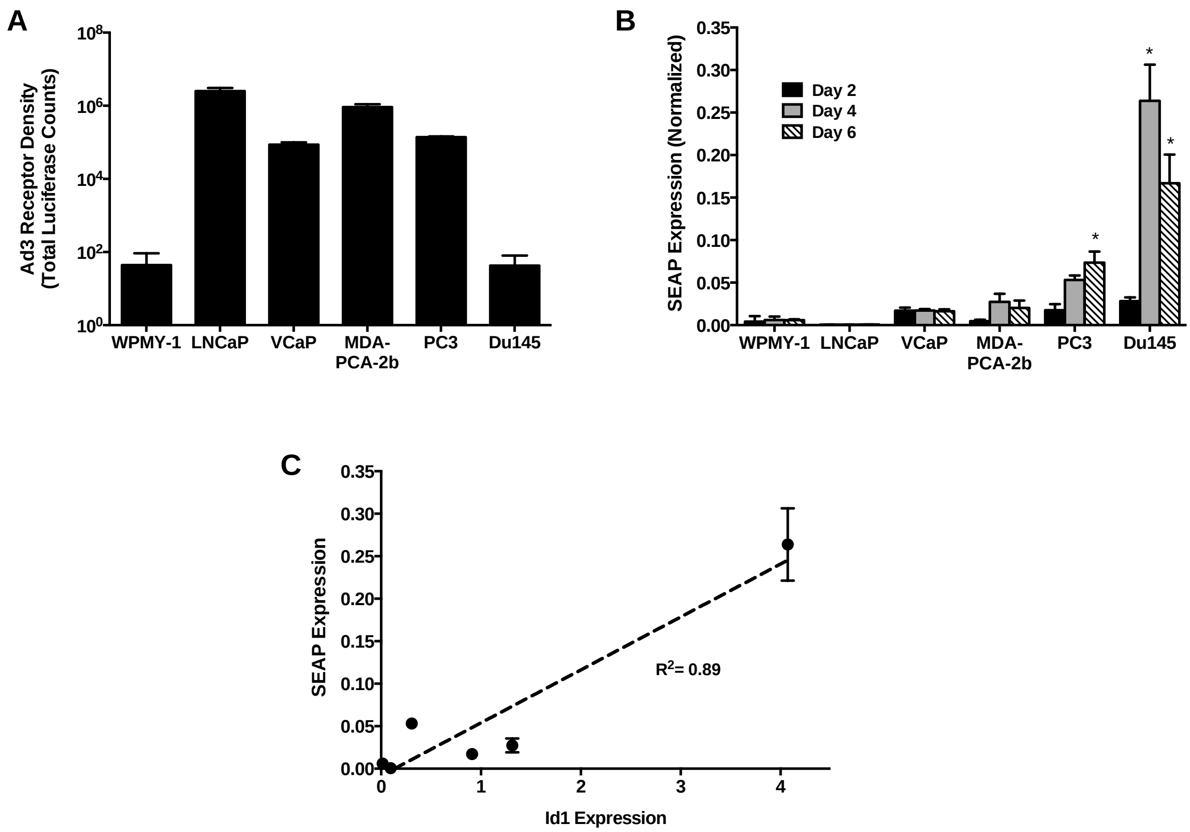

Figure 2. SEAP reporter expression increases with aggressiveness of prostate cancer cell and correlates with cellular level of Id1. (a) Ad3 receptor density for each cell type was determined following infection with an Ad5/3-CMV-Luc adenovirus (MOI=10). **(b)** SEAP reporter was measured in culture medium 2, 4 and 6 days post-infection with Ad5/3-Id1-SEAP-Id1-mCherry (MOI=1) and normalized with Ad3 receptor surface expression. *p<0.01 versus LNCap at corresponding timepoint. **(b)** Linear regression analysis was used to correlate SEAP reporter expression and cellular Id1. All data are reported as mean±SEM (n=4).

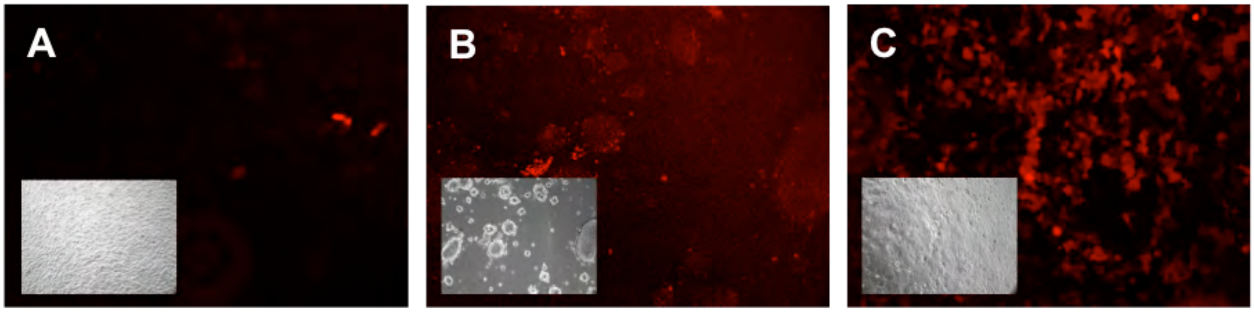

Figure 3. mCherry reporter fluorescence corresponds to prostate cancer cell aggressiveness. Representative fluorescence images of **(a)** normal prostate cells (WPMY-1) and cancerous cells with **(b)** moderate Id1 expression (VCaP) and **(c)** high Id1 expression (Du145). Inserts are corresponding bright field images. All images were acquired using a 10X objective.

Fluorescent mCherry reporter allows for *in vivo* localization of aggressive and non-aggressive tumors

Two days after flank implantation of Ad5/3-Id1-SEAP-Id1-mCherry-infected PC3 and LNCaP cells, the mCherry reporter protein was fluorescently detected. Representative images of mCherry expression illustrate that aggressive PC3 cells were visually detected at both low (Figure 4a) and high (Figure 4b) levels of total cell infectivity (2.5% and 17.5% of total tumor cells, respectively). Non-aggressive LNCaP cells were also detected at higher levels of infectivity (Figure 4d), however, mCherry fluorescence was not observable when only 2.5% of the total cells were infected (Figure 4c). Quantification of mCherry fluorescence with ROI analyses confirmed that reporter intensity corresponded to cancer cell aggressiveness and total infectivity since the most significant fluorescence was observed with the aggressive PC3 cells at 17.5% total infectivity (Figure 4e).

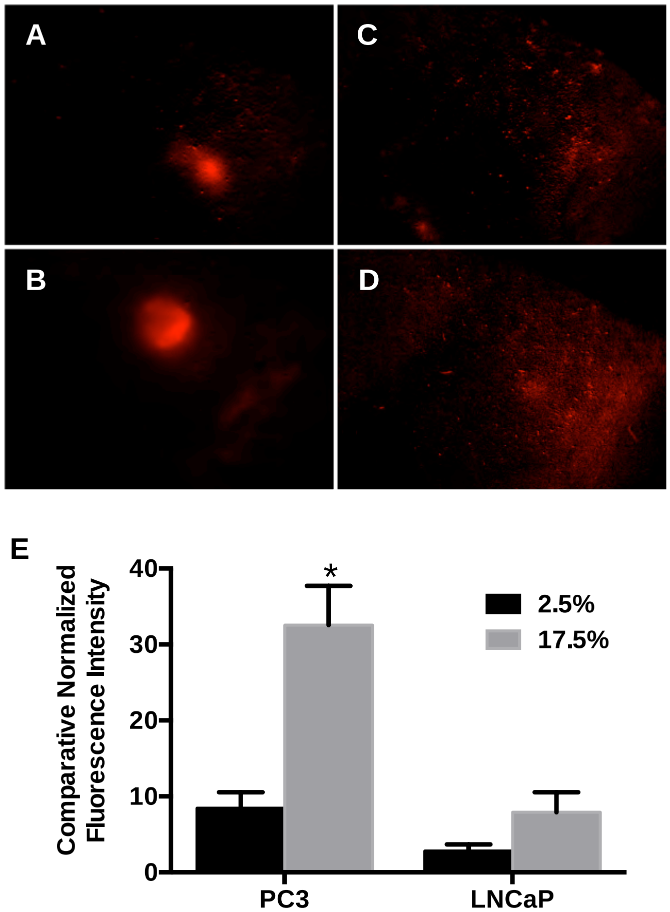

Figure 4. Infected tumors are visualized *in vivo* with the fluorescent mCherry reporter. (a-d) Representative images of mCherry reporter expression 2 days after flank implantation of PC3 **(a,b)** and LNCaP **(c,d)** cells with 2.5% **(a,c)** and 17.5% **(b,d)** total cell infectivity. PC3 and LNCaP cells were infected with Ad5/3-Id1-SEAP-Id1-mCherry for 24h and then implanted with non-infected cells to simulate low (2.5%) or high (17.5%) tumor infectivity. **(e)** Quantitative region of interest analysis of tumor fluorescence was done to measure mCherry reporter intensity following implantation. All data are reported as mean±SEM (n=4). **p*<0.001 versus all groups.

DISCUSSION

In the current work, a dual reporter vector, Ad5/3-Id1-SEAP-Id1-mCherry, was evaluated for its ability to noninvasively detect and monitor prostate cancer using expression of a SEAP reporter for blood-based detection and mCherry reporter for fluorescence imaging. Reporter expression of the diagnostic system was driven by the cancer-specific expression of Id1, which is a documented indicator of tumor malignancy with no expression found in BPH and normal prostate tissue [11-15, 24-28]. The present study used a panel of prostate cancer cells with varying degrees of reported aggressiveness in addition to normal prostate cells. Measurement of cellular levels of Id1 was used to quantify aggressiveness, allowing us to assess the relationship between cancer malignancy and diagnostic efficacy of the Ad5/3-Id1-SEAP-Id1-mCherry vector. Unlike measurements of PSA, which showed no correlation with cellular Id1, expression of the blood-based SEAP reporter showed a significant correlation with cancer cell aggressiveness.

Implantation of infected, tumor-forming cells demonstrated that the Ad5/3-Id1-SEAP-Id1-mCherry diagnostic vector can be used for *in situ* detection and localization of prostate cancer. By simulating low (2.5%) and high (17.5%) tumor cell infectivity, we demonstrated sensitive visualization of tumors formed by both aggressive (PC3) and non-aggressive (LNCaP) prostate cancer cells. Fluorescent mCherry reporter expression was detected in aggressive tumors with both high and low infectivity and non-aggressive tumors with high infectivity. The lower limit of detection for tumor visualization using mCherry fluorescence, however, was approached with poorly infected, non-aggressive LNCaP tumors. Since reporter expression is dependent on cellular Id1 expression and LNCaP cells have relatively low levels of Id1, greater tumor infectivity is needed for accurate localization.

The dependency of the diagnostic vector on adequate expression of Id1 represents a limitation of the current system for detecting less aggressive cancers. However, by achieving targeted delivery and increased tumor infectivity, the visual detection limits of the diagnostic vector can be surpassed. Our future work will aim to develop strategies to target vector delivery and infectivity of both aggressive and non-aggressive prostate cancer to allow for sensitive localization to aid in tumor resection.

In conclusion, the present work introduces a novel strategy for detection and localization of prostate cancer that overcomes the current limitations of the PSA test to distinguish between aggressive cancer and indolent conditions like BPH. The correlation between reporter expression and cellular Id1 enables SEAP levels to be used as a predictive measure of prostate cancer aggressiveness and mCherry fluorescence as an aid for tumor visualization. This strategy would assist clinicians in the detection and treatment of prostate cancer and ultimately reduce the mortality associated with this disease.

EXPERIMENTAL METHODS

Cell Culture

The efficacy of the diagnostic vector was evaluated using six prostate cancer cell lines: WMPY-1, MDA-PCa-2b, VCaP, PC3, Du145, and LNCaP (American Type Culture Collection, Manassas, VA). Two commonly used prostate cell lines, (RWPE-1 and Ca-HPV-10), were excluded from the cell panel due to immortalization vector HPV-18 interaction with endogenous Id1 protein [29-31]. LNCaP cells were maintained in RPMI-1640 with 10% fetal bovine serum (FBS) and 1% L-glutamine. Du145 cells were grown in EMEM with 10% FBS and 1% L-glutamine. VCap cells were maintained in DMEM containing 10% FBS and 1% L-glutamine. WMPY-1 cells were grown in DMEM with 5% FBS and 1% L-glutamine. PC3 cells were grown in F12k basal medium with 10% FBS. MDA-PCa-2b cells were maintained in F12k basal medium containing 20% FBS, 25 ng/mL cholera toxin, 10 ng/mL mouse EGF, 5 nM phosphoethanolamine, 100 pg/mL hydrocortisone, 45 nM selenious acid and 5 µg/mL bovine insulin. All cells were cultured at 37°C and 5% CO_2. Cells were allowed to reach 75-90% confluency prior to passaging.

In Vitro Experiments

Cells (1.0×10^5 cells/cm^2) were plated in quadruplicate 24 h before infection with Ad5/3-Id1-SEAP-Id1-mCherry. Cells were infected at a multiplicity of infection (MOI) ratio of one, calculated based on the plaque-forming units using a standard agarose-overlay plaque assay. Media was collected at 2, 4, and 6 days post-infection and SEAP levels measured using the Great EscAPe SEAP™ Fluorescence Detection kit (Clontech Laboratories, Mountain View, CA). Media was also collected from uninfected cells to measure background fluorescence. In addition, PSA levels were quantified in the culture medium of each cell type by an enzyme-linked immunosorbent assay (ELISA) specific for human PSA (AbCam, Cambridge, MA).

In order to qualify SEAP reporter expression as a singular function of Id1 promotor activity, an Ad3 receptor normalization assay was performed using an Ad5/3-CMV-Luc adenovirus. This adenovirus was generated using the same Ad5/3 adenoviral backbone used to construct the Ad5/3-Id1-SEAP-Id1-mCherry adenovirus. For all cell lines, 1.0×10^5 cells were infected with Ad5/3-CMV-Luc (MOI=1). Forty-eight hours post infection, cells were imaged with an IVIS-100 CCD imaging system (Caliper Life Sciences, Mountain View, CA). Matched region of interest (ROI) analysis was performed using instrument software (Living Image 3.2) to quantify total luciferase counts per well. Luciferase counts represented a relative surface expression of the Ad3 receptor for each cell type and were subsequently used to normalize the SEAP measurements.

Western Blot

Protein lysates from all cell lines were collected with RIPA-modified buffer (Sigma-Aldrich) with 1% SDS and phosphatase inhibitors (1 mM sodium orthovanadate, 25 mM bglycerophosphate, 100 mM sodium fluoride) and protease inhibitors (10 mg/mL leupeptin, 10 mg/mL aprotinin, 1 mM PMSF). Protein lysates (15 μg, determined by Lowry assay) were separated with 4-12% bis-Tris electrophoresis gel (Life Technology, Carlsbad, CA), followed by transfer to PVDF membranes (Millipore Immobilon, Billerica, MA). Membranes were blocked with 5% bovine serum albumin and probed with rabbit monoclonal anti-mouse Id1, clone 195-14 (CalBioreagents, San Mateo, CA), followed by horseradish peroxidase-conjugated goat anti-rabbit Ig (SouthernBiotech, Birmingham, AL). All membranes were washed three times with TBST buffer for 20 min per wash. Id1 protein was visualized using chemiluminescent substrate (SuperSignal West Pico Chemiluminescent Substrate, ThermoScientific, Rockford, IL). Densitometry was performed using ImageJ software, and Id1 levels were normalized to the respective β-actin controls.

In vivo analyses

Athymic male nude mice were obtained from Frederick Cancer Research (Hartford, CT). Two prostate cells lines (LNCaP and PC3) were transfected with Ad5/3-Id1-SEAP-Id1-mCherry (MOI=10) for 24 h. Following transfection, cells were harvested, washed and counted. For each cell type, mice (n=4) were implanted with 5×10^4 infected cells (2.5% of total cells) and 1.95×10^6 of uninfected cells in the flank. A second group of mice were implanted with 3.5×10^5 infected cells (17.5% of total cells) and 1.65×10^6 uninfected cells in the flank. Appropriate numbers of infected and uninfected cells were mixed in the syringe prior to implantation. Two additional groups of mice (n=4) were implanted in the flank with 2×10^6 uninfected cells of each type to serve as an uninfected, tumor bearing control group. Tumor fluorescence in the control group served as background levels for statistical comparison. All groups were fluorescently imaged on day 2 post-implantation.

Fluorescence Imaging

Representative *in vitro* fluorescent images were acquired on day 2 post-infection with Ad5/3-Id1-SEAP-Id1-mCherry. Cell images (100x) were rendered using an mCherry 587 nm excitation/600 nm long pass filter on an inverted microscope with a halogen light source and Nuance multi-spectral camera (CRi, Woburn, WA). A liquid-crystal tunable wavelength filter in the camera was set for collection of emission images from 600 to 720 nm in 5-nm increments. Composite images (unmixed composites) were generated for each image cube by unmixing the spectral signature of the mCherry reporter from those of background auto-fluorescence. For *in vivo* images, mice were anesthetized with isoflurane and tumors were imaged with a Leica stereomicrosope (Model MZ-FLIII, Vashaw Scientific, Norcross, GA). Filter, camera, and image processing from the *in vitro* imaging methods were used in coordination with the stereomicroscope. Quantitative ROI analysis for mCherry fluorescence in tumors was performed with ImageJ software.

Statistical analyses

Results are reported as the mean plus or minus standard error of the mean (SEM). Data were analyzed for statistical significance by Student's *t*-test or analysis of variance (ANOVA) with Bonferroni's multiple comparison test where appropriate using Prism (version 6.0, GraphPad Software). For statistical analyses of PSA data, values for the normal prostate cells (WPMY-1) were used as a baseline PSA level and comparisons to baseline were made using

Student's *t*-test. For SEAP measurements, background fluorescence from uninfected cells was subtracted from the measured fluorescence of infected cells and SEAP levels were normalized to corresponding Ad3 receptor expression. Linear regression analyses were used to correlate SEAP and PSA levels with cancer cell aggressiveness (Id1 expression). For *in vivo* quantification of the mCherry reporter, fluorescence intensity of the infected tumors was normalized to Ad3 receptor expression and quantified as a fold-increase over the intensity of the matching ROI of the tumor-bearing control group.

1. Cancer Facts and Figures 2011. (2011). American Cancer Society. Atlanta, GA.

2. Jemal, A, Siegel, R, Ward, E, Murray, T, Xu, J, Smigal, C, *et al.* (2006). Cancer statistics, 2006. *CA: a cancer journal for clinicians* **56**: 106-130.

3. Grubb, RL, 3rd, Pinsky, PF, Greenlee, RT, Izmirlian, G, Miller, AB, Hickey, TP, *et al.* (2008). Prostate cancer screening in the Prostate, Lung, Colorectal and Ovarian cancer screening trial: update on findings from the initial four rounds of screening in a randomized trial. *BJU international* **102**: 1524-1530.

4. Schroder, FH, Hugosson, J, Roobol, MJ, Tammela, TL, Ciatto, S, Nelen, V, *et al.* (2009). Screening and prostate-cancer mortality in a randomized European study. *The New England journal of medicine* **360**: 1320-1328.

5. Abrahamsson, PA, Artibani, W, Chapple, CR, and Wirth, M (2009). European Association of Urology position statement on screening for prostate cancer. *European urology* **56**: 270-271.

6. Smith, RA, Cokkinides, V, Brooks, D, Saslow, D, and Brawley, OW (2010). Cancer screening in the United States, 2010: a review of current American Cancer Society guidelines and issues in cancer screening. *CA: a cancer journal for clinicians* **60**: 99-119.

7. Lin, K, Lipsitz, R, Miller, T, Janakiraman, S, and Force, USPST (2008). Benefits and harms of prostate-specific antigen screening for prostate cancer: an evidence update for the U.S. Preventive Services Task Force. *Annals of internal medicine* **149**: 192-199.

8. Sun, XH, Copeland, NG, Jenkins, NA, and Baltimore, D (1991). Id proteins Id1 and Id2 selectively inhibit DNA binding by one class of helix-loop-helix proteins. *Molecular and cellular biology* **11**: 5603-5611.

9. Pesce, S, and Benezra, R (1993). The loop region of the helix-loop-helix protein Id1 is critical for its dominant negative activity. *Molecular and cellular biology* **13**: 7874-7880.

10. Yu, X, Xu, X, Han, B, and Zhou, R (2009). Inhibitor of DNA binding-1 overexpression in prostate cancer: relevance to tumor differentiation. *Pathology oncology research : POR* **15**: 91-96.

11. Ouyang, XS, Wang, X, Lee, DT, Tsao, SW, and Wong, YC (2002). Over expression of ID-1 in prostate cancer. *The Journal of urology* **167**: 2598-2602.

12. Ouyang, XS, Wang, X, Lee, DT, Tsao, SW, and Wong, YC (2001). Up-regulation of TRPM-2, MMP-7 and ID-1 during sex hormone-induced prostate carcinogenesis in the Noble rat. *Carcinogenesis* **22**: 965-973.

13. Darby, S, Cross, SS, Brown, NJ, Hamdy, FC, and Robson, CN (2008). BMP-6 over-expression in prostate cancer is associated with increased Id-1 protein and a more invasive phenotype. *The Journal of pathology* **214**: 394-404.

14. Ling, MT, Wang, X, Lee, DT, Tam, PC, Tsao, SW, and Wong, YC (2004). Id-1 expression induces androgen-independent prostate cancer cell growth through activation of epidermal growth factor receptor (EGF-R). *Carcinogenesis* **25**: 517-525.

15. Zhang, X, Ling, MT, Wang, X, and Wong, YC (2006). Inactivation of Id-1 in prostate cancer cells: A potential therapeutic target in inducing chemosensitization to taxol through activation of JNK pathway. *International journal of cancer Journal international du cancer* **118**: 2072-2081.

16. Shaner, NC, Campbell, RE, Steinbach, PA, Giepmans, BN, Palmer, AE, and Tsien, RY (2004). Improved monomeric red, orange and yellow fluorescent proteins derived from Discosoma sp. red fluorescent protein. *Nature biotechnology* **22**: 1567-1572.

17. Warram, JM, Borovjagin, AV, and Zinn, KR (2011). A genetic strategy for combined screening and localized imaging of breast cancer. *Molecular imaging and biology : MIB : the official publication of the Academy of Molecular Imaging* **13**: 452-461.

18. Bello, D, Webber, MM, Kleinman, HK, Wartinger, DD, and Rhim, JS (1997). Androgen responsive adult human prostatic epithelial cell lines immortalized by human papillomavirus 18. *Carcinogenesis* **18**: 1215-1223.

19. Papsidero, LD, Kuriyama, M, Wang, MC, Horoszewicz, J, Leong, SS, Valenzuela, L, *et al.* (1981). Prostate antigen: a marker for human prostate epithelial cells. *Journal of the National Cancer Institute* **66**: 37-42.

20. Kaighn, ME, Narayan, KS, Ohnuki, Y, Lechner, JF, and Jones, LW (1979). Establishment and characterization of a human prostatic carcinoma cell line (PC-3). *Investigative urology* **17**: 16-23.

21. Korenchuk, S, Lehr, JE, L, MC, Lee, YG, Whitney, S, Vessella, R, *et al.* (2001). VCaP, a cell-based model system of human prostate cancer. *In vivo* **15**: 163-168.

22. Navone, NM, Olive, M, Ozen, M, Davis, R, Troncoso, P, Tu, SM, *et al.* (1997). Establishment of two human prostate cancer cell lines derived from a single bone metastasis. *Clinical cancer research : an official journal of the American Association for Cancer Research* **3**: 2493-2500.

23. Gibas, Z, Becher, R, Kawinski, E, Horoszewicz, J, and Sandberg, AA (1984). A high-resolution study of chromosome changes in a human prostatic carcinoma cell line (LNCaP). *Cancer genetics and cytogenetics* **11**: 399-404.

24. Wong, YC, Wang, X, and Ling, MT (2004). Id-1 expression and cell survival. *Apoptosis : an international journal on programmed cell death* **9**: 279-289.

25. Sikder, HA, Devlin, MK, Dunlap, S, Ryu, B, and Alani, RM (2003). Id proteins in cell growth and tumorigenesis. *Cancer cell* **3**: 525-530.

26. Ling, MT, Lau, TC, Zhou, C, Chua, CW, Kwok, WK, Wang, Q, *et al.* (2005). Overexpression of Id-1 in prostate cancer cells promotes angiogenesis through the activation of vascular endothelial growth factor (VEGF). *Carcinogenesis* **26**: 1668-1676.

27. Ouyang, XS, Wang, X, Ling, MT, Wong, HL, Tsao, SW, and Wong, YC (2002). Id-1 stimulates serum independent prostate cancer cell proliferation through inactivation of p16(INK4a)/pRB pathway. *Carcinogenesis* **23**: 721-725.

28. Forootan, SS, Wong, YC, Dodson, A, Wang, X, Lin, K, Smith, PH, *et al.* (2007). Increased Id-1 expression is significantly associated with poor survival of patients with prostate cancer. *Human pathology* **38**: 1321-1329.

29. Alani, RM, Hasskarl, J, Grace, M, Hernandez, MC, Israel, MA, and Munger, K (1999). Immortalization of primary human keratinocytes by the helix-loop-helix protein, Id-1. *Proceedings of the National Academy of Sciences of the United States of America* **96**: 9637-9641.

30. Yasmeen, A, Bismar, TA, Kandouz, M, Foulkes, WD, Desprez, PY, and Al Moustafa, AE (2007). E6/E7 of HPV type 16 promotes cell invasion and metastasis of human breast cancer cells. *Cell cycle* **6**: 2038-2042.

31. Akil, N, Yasmeen, A, Kassab, A, Ghabreau, L, Darnel, AD, and Al Moustafa, AE (2008). High-risk human papillomavirus infections in breast cancer in Syrian women and their association with Id-1 expression: a tissue microarray study. *British journal of cancer* **99**: 404-407.

References: Publications and Abstracts:

1. Sorace AG, Warram JM, Mahoney M, Zinn KR, **Hoyt K**. Enhancement of adenovirus delivery after ultrasound-stimulated therapy in a cancer model. Ultrasound in Medicine and Biology, 2013
2. Sorace AG, Mahoney M, Zinn KR, **Hoyt K**. Volumetric molecular ultrasound imaging of tumor vascularity in a preclinical model of prostate cancer. American Institute for Ultrasound in Medicine Annual Convention, 32:S16, 2013.

Appendices:

Appendix I: Richter JR, Mahoney M, Warram JM, Samuel S, Zinn KR. A Dual-reporter, Diagnostic Vector For Detection and Localization of Prostate Cancer. *Mol Ther.* In preparation.
Appendix II: Sorace AG, Warram JM, Mahoney M, Zinn KR, Hoyt K. Enhancement of adenovirus delivery after ultrasound-stimulated therapy in a cancer model. Ultrasound in Medicine and Biology, 2013 (In press).

Enhancement of Adenovirus Delivery after Ultrasound-Stimulated Therapy in a Cancer Model

Anna G. Sorace[1], Jason M Warram[2], Marshall Mahoney[1], Kurt R Zinn[1,2,3,4], Kenneth Hoyt[1,2,3,4]

Departments of Biomedical Engineering[1], Radiology[2], Electrical & Computer Engineering[3], and Comprehensive Cancer Center[4], University of Alabama at Birmingham, Birmingham, AL USA

Corresponding author:

Kenneth Hoyt, PhD, MBA, University of Alabama at Birmingham, Volker Hall G082, 1670 University Boulevard, Birmingham, AL 35294 USA

Ph: (205) 934-3116

Fx: (205) 975-6522

Email: hoyt@uab.edu

Running title: Ultrasound-stimulated adenovirus delivery

ABSTRACT

Improving the efficiency of adenovirus (Ad) delivery to target tissues has the potential to advance the translation of cancer gene therapy. Ultrasound (US)-stimulated therapy utilizes microbubbles (MBs) exposed to low-intensity US energy to improve localized delivery. We hypothesize that US-stimulated gene therapy can improve Ad infection in a primary prostate tumor through enhanced tumor uptake and retention of the Ad vector. *In vitro* studies were performed to analyze the degree of Ad infectivity after application of US-stimulated gene therapy. A luciferase-based Ad on a ubiquitous cytomegalovirus (CMV) promoter (Ad5/3-CMV-Luc) was used in an animal model of prostate cancer (bilateral tumor growth) to evaluate Ad transduction efficiency after US-stimulated therapy. Bioluminescence imaging was employed for *in vivo* analysis to quantify Ad infection within the tumor. *In vitro* studies revealed no difference in Ad transduction between groups receiving US-stimulated therapy using high, low, or sham US intensity exposures at various multiplicity of infections (MOIs) (p = 0.80). *In vivo* results showed that tumors receiving US-stimulated therapy after intratumoral injection of Ad5/3-CMV-Luc (1 x 10^6 plaque forming units) demonstrated a 73.6% enhancement in tumor delivery and retention compared to control tumors receiving sham US (p = 0.03). US-stimulated therapy has significant potential to immediately impact Ad-based cancer gene therapy by improving virus bioavailability in target tissues.

Key words: cancer; gene therapy; microbubble contrast agent; ultrasound

INTRODUCTION

There is an urgent need to improve delivery of recombinant adenovirus (Ad) in order to advance cancer gene therapy. Ad vectors show immense potential in cancer therapy due to their ability to selectively target and destroy specific tumor cells, while not injuring healthy tissue. Multiple applications using Ad vectors in cancer have been explored. Therapeutic strategies often involve the triggering of cell death via a death-inducing reporter that is specifically driven by a cancer promoter. Other utilities involve immunotherapeutic approaches aimed at inducing host antitumor immune responses (Lupold and Rodriguez 2005). Direct cancer cell death can be accomplished through delivery of replication oncolytic viruses or non-replicating vectors encoding tumor suppressor genes, suicide genes, or antiangiogenic genes (Kaplan 2005). Tumor cells can be destroyed at both primary and metastatic locations through induction of host antitumor immune responses. Although gene therapy has advanced in the last decade, there are many limitations that prevent routine applications. The effectiveness of gene therapy is directly dependent on successful site-specific delivery. Limitations of delivery include anti-Ad host immune response, tumor cell transduction, extravasation of the large molecules to their intended site, and the ubiquitous Ad receptor can lead to virus uptake in cell types other than the targeted region. Additional hurdles include the inability to overcome filtration from the liver, and the limited infectivity of Ad serotype 5 (Ad5). These limitations lead to necessary advancements in the field of Ad delivery.

US-stimulated therapy provides a localized technique to enhance agent delivery. MBs are clinically used US contrast agents have proven to be non-immunogenic and non-toxic in nature (Calliada et al. 1998; Cosgrove 2006). This unique therapy uses US-exposed MBs to both increase cell membrane permeability and induce localized molecular extravasation (Dijkmans et al. 2004; Ferrara et al. 2007; Lindner 2004; Song et al. 2002; Sorace et al. 2012). Although there is some disputing evidence between the exact duration of this effect, this therapeutic stimulation has been shown to last up to 30 minutes post US exposure (Sorace et al. 2013). US-stimulated therapy has been increasingly popular in preclinical models because it is generally noninvasive and has significant potential for translation. US-stimulated therapy has been shown to increase cytotoxic agent delivery to cancer to improve response by greater than 50% compared to drug alone (Casey et al. 2010; Heath et al. 2012; Sorace et al. 2012). It has also been demonstrated that positive effects can be achieved after only a single dose of treatment (Sorace et al. 2013). Other applications of this therapy include delivery of drugs through the blood-brain barrier and enhancing delivery of DNA (Klibanov 2006; McDannold et al. 2012; Sirsi and Borden 2012; Treat et al. 2012). Studies have also shown that Ad particles can be safely delivered to a localized region by MB packaging to avoid ubiquitous uptake in other cells and liver filtration (Warram et al. 2012). To the best of our knowledge, applying US-stimulated therapy to enhanced Ad delivery is a novel application of this US technology.

In order to establish genetic-based therapeutics as a routine treatment option for cancer patients, delivery barriers must be overcome (de Vrij et al. 2010). In the current study, US-stimulated therapy is evaluated for the potential to improve Ad vector transduction in an animal model of prostate cancer. Considering the relatively safe properties associated with US-stimulated therapy, positive evaluation of this technique could immediately impact Ad-based therapy trials leading to improved treatment success and patient survival.

MATERIALS AND METHODS

Adenovirus Preparation

A non-replicative, luciferase-reporter based, serotype 5 Ad on a ubiquitous cytomegalovirus (CMV) promoter (Ad5/3-CMV-Luc) was used to evaluate Ad transduction due to the ease of bioluminescence imaging for evaluation of response. In order to improve infectivity and ablate coxsackie Ad receptor (CAR) mediated infection, the Ad5/3-CMV-Luc contains a serotype chimeric infectivity motif where the serotype 3 Ad (Ad3)-specific tropism conferred to the Ad serotype 5 fiber by its knob domain replacement with that of the Ad3 fiber. For the study, particle amplification was performed in HEK-293 cells and purified using cesium chloride centrifugation gradients. A standard agarose-overlay plaque assay was conducted with HEK-293 cells to determine a viral titer of 1.1×10^{11} plaque forming units (PFU) per mL.

Cell Culture

PC3 human prostate cancer cells were purchased from the American Tissue Type Collection (Manassas, VA, USA)**.** The cell line was maintained in DMEM media with 10% FBS and 1% L-glutamine. All cells were grown to 80 to 90% confluence before passaging. Cell numbers were determined using a standard hemocytometer and cell viability was measured by trypan blue dye exclusion.

In Vitro Experimentation

Experiment 1: Aliquots (0.1 mL in PBS) of Ad5/3-CMV-Luc were placed in 1.5 mL polypropylene microcentrifuge tubes at various PFU amounts (0, 3.5, 3.5×10^1, 3.5×10^2, and 3.5×10^3 infectious virus particles). Groups were then subdivided into low-pressure US, high-pressure US, and sham US exposure (control) groups. All groups were evaluated in triplicate. To each tube, 10 μL of MBs (Definity, Lantheus Medical Imaging, North Billerica, MA, USA) was added immediately prior to US-stimulated therapy. US exposure was performed on the groups in a 37°C water bath with the following acoustic parameters: 1.0 MHz transmit frequency, peak negative pressures of 0.85 MPa (high pressure condition) or 0.1 MPa (low pressure condition), a pulse repetition period of 0.1 sec, 10% duty cycle, and a 5 min duration of US exposure. An unfocused single-element (0.75 inch) immersion transducer (Olympus, Waltham, MA, USA) was placed in series with a signal generator (AFG3002B, Tektronix, Beaverton, OR, USA) and power amplifier (A075, Electronics and Innovation, Rochester, NY, USA). Ad groups were then added at various multiplicity of infection (MOI) ratios (0, 0.01, 0.1, 1, and 10) to PC3 cells (3.5×10^2 cells per well in a 24 black well plate) plated 24 hr prior. Note that an MOI value is defined as the ratio of Ad particles to infectious targets (i.e., number of cells per well). Virus aliquots were allowed to incubate for 1 hr then removed and replaced with complete media.

Luciferin (2.5 mg) was diluted into 25 mL of PBS. Media was removed from the plates and replaced with 1 mL of diluted luciferin (100 µg) per well to oversaturate the cells. Following a 24 hr incubation period (after Ad vector exposure), bioluminescence imaging was performed using the IVIS-100 System (Xenogen Corporation, Hopkinton, MA, USA) with an image acquisition time of 300 sec (binning of 8 and f/stop of 1) at a fixed stage height. A region-of-interest (ROI) was drawn around each well and the bioluminescence signal was summarized as total photon counts using equipment software.

Experiment 2: Aliquots (0.1 mL in PBS) of PC3 cells (3.5 x 10^2) and Ad5/3-CMV-Luc (3.5 x 10^2 PFU, MOI = 1) in polypropylene microcentrifuge tubes underwent high pressure US treatment (N = 13) or sham US treatment (N = 13) in the presence of MBs in a 37°C water bath using identical high pressure US parameters as experiment 1. After applying US therapy, cells and Ad were plated in a 24 well plate, and then rinsed and replaced with complete media after 1 hr. Twenty-four hr thereafter, plates were imaged for presence of bioluminescence as described in the previous section.

In Vivo Experimentation

Animal studies were approved by the Institute of Animal Care and Use Committee (IACUC) at the University of Alabama at Birmingham. PC3 cancer cells (2 x 10^6 cells per 100 µL DMEM media without FBS) were implanted subcutaneously in bilateral flanks of five-week-old nude athymic male mice (Frederick Cancer Research, Hartford, CT, USA) (N = 24 animals, N = 48 tumors). Tumors were allowed to grow approximately five weeks to equal tumor size according to caliper measurements (final tumor size of 34.1 ± 2.8 mm^2). Each animal received a 30 µL tail vein injection of MBs (Definity) diluted to a final volume of 100 µL with saline. Animals were then submerged in a custom-built 37ºC water bath and remained under isoflurane gas anesthesia for the entirety of the US-stimulated therapy. Two min post MB injection, US exposure was applied to the left flank tumor. Right tumors did not receive US treatment. US-stimulated therapy was performed using the previously detailed parameters. This setup allowed exposure of the entire target tumor with US energy while the contralateral tumor was outside the path of US transmission. Immediately following US, the Ad5/3-CMV-Luc vector was injected intratumorally in both bilateral flank tumors. Animals were divided into three groups and dosed with different Ad concentrations: 1 x 10^6 PFU (N = 12), 1 x 10^7 PFU (N = 5), and 1 x 10^9 PFU (N = 7). For the remainder of the manuscript, 1 x 10^6, 1 x 10^7, and 1 x 10^9 will be referred to as the “low”, “medium”, and “high” concentrations of Ad injection, respectively. Intratumoral doses were administered in total volume of 50 µL. Animals were imaged for bioluminescence expression before therapy on day 0 (baseline) and again on day 2 (48 hours post therapy) using the following methods. Animals were injected intraperitoneal (IP) with firefly luciferin (2.5 mg) which reacts with the luciferase enzyme to produce a bioluminescence reporter signal following luciferase gene expression. After a 15 min period allowing for systemic circulation, all animals were oriented so both tumors were visualized and then imaged for bioluminescence expression using the IVIS-100 System (Xenogen Corporation) and established data acquisition protocols. Five animals were imaged simultaneously using a 300 see exposure, f/stop of 1, binning of 8, and fixed stage height. Standardized ROIs were generated using instrument software to analyze photon counts.

Statistical Analysis

All experimental data was summarized as mean ± SE and reported as percent change or bioluminescence counts. A 2-sample paired *t*-test was used to calculate statistical difference between control and US-stimulated tumors within each group. No comparisons were done directly between the various Ad concentration groups. A *p*-value of less than 0.05 was considered statistically significant. Analyses were completed using the SAS statistical software package (Cary, NC, USA).

RESULTS

During *in vitro* experiment 1, various concentrations of Ad particles were exposed to US-stimulated therapy in the absence of cells to determine the effect of US treatment on the infectivity potential of the virus. After US exposure, the Ad was added to plated cells at various MOIs and allowed in incubate. Bioluminescence imaging resulting from successful Ad infection demonstrated that there is no significant difference in virus infectivity or vector transduction at high, low, or no (sham) exposure to US pressures (p = 0.80), Figure 1. The importance of this finding is that it confirms that exposing the Ad vector to US intensity levels necessary for inducing membrane permeabilization during US-stimulated therapy has no negative effect on the infectivity potential of the Ad. The various MOIs tested confirm that this observation was consistent across various concentrations of Ad.

For *in vitro* experiment 2, Ad particles received US-stimulated therapy in the presence of PC3 cells (MOI = 1) to determine effects of US treatment on cellular response to infection. The control group contained Ad5/3-CMV-Luc, cancer cells, and MBs without US treatment. Figure 1 demonstrates that there was no difference in bioluminescence expression when measured after Ad infection in the therapy group ($5.4 \times 10^5 \pm 1.9 \times 10^4$ counts) and control group ($5.3 \times 10^5 \pm 2.0 \times 10^4$ counts) (p = 0.92). These results suggest that there was no cellular internalization of the Ad. US-stimulated therapy induced neither negative nor positive effects when applied to a combination of MBs, cells and Ad.

Analysis of US-stimulated gene therapy effects on Ad5/3-CMV-Luc transduction in an *in vivo* model of prostate cancer was also performed. Bilateral flank tumors were used in order to provide *in situ* control tumors that did not receive US exposure. After US-stimulated therapy was applied to treatment tumors, Ad5/3-CMV-Luc was immediately administered to the three animal groups via an intratumoral injection using low, moderate, and high Ad concentrations. Forty-eight hr post treatment, the low concentration therapy group showed a 95.1 ± 35.1% increase in bioluminescence expression compared to control (p = 0.03). At the moderate concentration, the therapy group exhibited a 12.1 ± 6.4% increase compared to control, trending towards significance (p = 0.06). Finally, at the high concentration, the therapy group exhibited no difference compared to control group showing a 10.1 ± 22.8% increase (p = 0.09), Figure 2. A qualitative analysis shows the visual differences in overall bioluminescence expression between therapy and control tumors of low, moderate, and high Ad concentration groups at baseline and 48 hours. Figure 2 also shows representative bioluminescence images exhibiting enhancement of infectivity at 48 hr in the tumors receiving US-stimulated therapy compared to the contralateral control tumor and baseline images. Further analysis of the low Ad concentration group revealed that at baseline, there were no statically significant differences between the control and US therapy exposed tumors (p = 0.27). Individual analysis of the animals in the low concentration Ad group demonstrates that 75% of the animals studied revealed increased infectivity, 17% showed relatively no change, and one animal exhibited a negative response, Figure 3.

DISCUSSION

Enhanced tissue-specific delivery of Ad-based vectors has the potential to make significant improvements to current cancer gene therapy protocols. The strategies investigated here provide original advances in Ad delivery to the intended region to assist virus retention within the target tumor tissue. The *in vitro* studies confirmed that Ad infectivity was not affected by either the high or low US pressure conditions (1.0 MHz frequency). While the approach in this study was to inject the virus post US-stimulated therapy, evaluating the effects of US-stimulated therapy directly on Ad particles was necessary for future translation and investigations. For future work utilizing either a multi-dose study or intratumoral injections administered prior to therapy, we can be confident that we are not altering the gene therapy vector during exposure to US energy levels detailed in this article.

Internalization of the Ad vector, which ultimately leads to tissue infection, is triggered by interaction of the viral penton with epithelial integrins. From there it is processed to the nucleus and is eventually expressed (Lupold and Rodriguez 2005). The Ad requires receptor-mediated internalization therefore intracellular delivery through membrane permeabilization could decrease expression. *In vitro* experiments demonstrated that increased Ad transduction did not occur and therefore was not due to increased infection by altering the mechanisms of the adenoviral process or internalization. This is consistent with previous studies analyzing gene transfer with US-stimulated therapy (Miller and Quddus 2000; Price et al. 1998). Bioluminescence signal measurements between *in vitro* experiments shows precision of infection at an MOI of 1. US alone has the capacity to increase the surrounding medium's temperature, which could potentially alter infection rate however there was no change in water bath temperature as monitored throughout the entirety of each US treatment session. No differences were found in Ad infectivity *in vitro* when US-stimulated therapy was applied directly to cells. Previous experiments have shown that no decreases in cell viability occurs during similar US-stimulated conditions (Sorace et al. 2012). The MOI of 1 was chosen for this experiment to not oversaturate the cells in order to more accurately evaluate and quantify interactions between cells and Ad. Considering receptor-mediated internalization required for successful virus infection, US-induced internalization would not lead to reporter transduction. Therefore, if a decrease in bioluminescence signal was observed within the US group, it would indicate the viral particles were sequestered inside the cell and not available for traditional infection. Since this was not observed, the conclusion is that US-stimulated internalization did not occur. It is proposed that the large size of the Ad vector compared to drug molecules decreases its ability to be internalized through a membrane permeabilization effect from US-stimulated therapy.

Detailed *in vivo* studies evaluated enhancement of Ad delivery after applying US-stimulated therapy in an animal model of prostate cancer. The greatest enhancement of Ad transduction was observed at the lowest vector dose, while little or no change was observed at the highest doses. At the highest dose, Ad availability at the cancer cell level was not a boundary for transduction due to the high concentration (tissue saturation) of the Ad vector. Considering the purpose of the study was to highlight enhanced transduction from US-stimulated therapy, the lowest dose provided the greatest potential for improvement. Although 75% of the animals studied demonstrated a positive outcome when administered a low concentration of Ad in combination with US-stimulated therapy, there was one animal which demonstrated a decrease in Ad tumor delivery. The animal showing a negative response could potentially be a result of a poor intratumoral injection. Notwithstanding, the utilization of this promising US technology would improve the bioavailability of low Ad vector doses and allow a lower dose to achieve the same therapeutic effect as high dose administrations. This outcome could help reduce patient toxicity, which currently hinders widespread use of gene therapy techniques in the clinic. As opposed to intravenous injections, intratumoral injections can offset the limitations of adenoviral gene delivery such as the anti-Ad host immune response and the ubiquitous Ad receptor leading to adenoviral uptake in all cell types.

Several studies have been detailed in the literature that investigated gene transfection efficiency in various tissue types using Ad vectors enhanced by US-stimulated delivery techniques. Specifically, the efficacy and safety of multidrug resistance 1 (MDR1) gene transfer into bone marrow cells was recently shown in a series of *in vitro* experiments to be enhanced using US-stimulated therapy (Guo et al. 2011). Another research group integrated plasmid DNA into a MB shell once the injected agents reached the target tumor tissue, high-intensity US energy was used to destroy the MBs and trigger localized payload (DNA) delivery (Sirsi et al. 2012). Using bioluminescence imaging techniques, this group was able to detect a significantly higher region of expression within the tumor compared to normal tissue. Research analyzing the longitudinal effects of antiangiogenic gene therapy on hepatocellular carcinoma demonstrated a significant decrease in microvessel density and increase in apoptosis using US-stimulated therapy with plasmid compared to plasmid alone (Nie et al. 2008). Various other studies have investigated US-stimulated delivery of genetic material in the heart (Bekeredjian et al. 2005; Shohet et al. 2000; Tsunoda et al. 2005), pancreas (Chen et al. 2006), skeletal muscle (Wang et al. 2005; Zhang et al. 2006), kidney (Koike et al. 2005), central nervous system (Shimamura et al. 2005), and solid tumors (Nie et al. 2008; Wang et al. 2009; Warram et al. 2012).

There are phase I and II trials currently ongoing to evaluate Ad vector delivery in human. Ad vectors are being explored due to their high transduction efficiency compared to a retrovirus or lentivirus. Phase II clinical studies in Ad-based prostate-specific antigen (PSA) vaccine are also being conducted. The PSA vaccine has been deemed safe with minimal toxicity side effects compared to more conventional anticancer drugs and the investigators hope that the Ad vector will produce immunity to the PSA and destroy cancer cells producing PSA (NCT00583024) (Department of Defense 2007). Along with the vaccines that are being studied, there is also a phase I trial utilizing an Ad5.SSTR/TK.RGD gene therapy vector, which is an infectivity-enhanced Ad that expresses a therapeutic thymidine kinase (TK) suicide gene and a somatostatin receptor (SSTR) for imaging patients with recurrent gynecologic cancer. When used in combination with a chemotherapeutic drug (ganciclovir), this novel Ad vector has been shown to induce cancer cell apoptosis (Kim et al. 2012). This particular study utilized an Ad for imaging gene transfer and monitoring therapeutic response and represents one of the first studies of its kind to prove safety and efficacy in human. Notwithstanding, these authors noted that further refinements in enhancing Ad vector infectivity are needed. Incorporation of US-stimulated gene therapy may help overcome this problem.

The ability to protect Ad vectors from systemic clearance and liver retention while enhancing its bioavailability within the tumor are important advancements in gene delivery to the target tumor. Previous research has shown that US-stimulated therapy can enhance delivery of both drugs and plasmids for cancer treatment. To the best of our knowledge, this article details the first study utilizing US-stimulated therapy to improve Ad delivery to the target tumor. Our results illustrating that Ad infection can be considerably enhanced after a single session of US-stimulated therapy is a significant finding in the field of cancer gene therapy and warrants further investigation.

ACKNOWLEDGEMENTS

The authors would like to thank Anton Borovjagin, PhD, from the School of Dentistry at the University of Alabama at Birmingham (UAB) for the generous donation of the Ad vector used in this article. This research project was supported in part by grant number PC111230 from the Prostate Cancer Research Program of the Department of Defense and a pilot award from the Department of Radiology at UAB.

REFERENCES

Bekeredjian R, Grayburn PA, Shohet RV, Use of ultrasound contrast agents for gene or drug delivery in cardiovascular medicine. J Am Coll Cardiol 2005; 45:329-35.

Calliada F, Campani R, Bottinelli O, Bozzini A, Sommaruga MG, Ultrasound contrast agents: basic principles. Eur J Radiol 1998; 27 Suppl 2:S157-60.

Casey G, Cashman JP, Morrissey D, Whelan MC, Larkin JO, Soden DM, Tangney M, O'Sullivan GC, Sonoporation mediated immunogene therapy of solid tumors. Ultrasound Med Biol 2010; 36:430-40.

Chen S, Ding JH, Bekeredjian R, Yang BZ, Shohet RV, Johnston SA, Hohmeier HE, Newgard CB, Grayburn PA, Efficient gene delivery to pancreatic islets with ultrasonic microbubble destruction technology. Proc Natl Acad Sci U S A 2006; 103:8469-74.

Cosgrove D, Ultrasound contrast agents: an overview. Eur J Radiol 2006; 60:324-30.

de Vrij J, Willemsen RA, Lindholm L, Hoeben RC, Bangma CH, Barber C, Behr JP, Briggs S, Carlisle R, Cheng WS, Dautzenberg IJ, de Ridder C, Dzojic H, Erbacher P, Essand M, Fisher K, Frazier A, Georgopoulos LJ, Jennings I, Kochanek S, Koppers-Lalic D, Kraaij R, Kreppel F, Magnusson M, Maitland N, Neuberg P, Nugent R, Ogris M, Remy JS, Scaife M, Schenk-Braat E, Schooten E, Seymour L, Slade M, Szyjanowicz P, Totterman T, Uil TG, Ulbrich K, van der Weel L, van Weerden W, Wagner E, Zuber G, Consortium G, Adenovirus-derived vectors for prostate cancer gene therapy. Hum Gene Ther 2010; 21:795-805.

Department of Defense UoI. Phase II Study of Adenovirus/PSA Vaccine in Men With Hormone - Refractory Prostate Cancer (APP22): Bethesda (MD): National Library of Medicine (US). Available from: http://clinicaltrials.gov/show/NCT00583024 NLM Identifier: NCT00583024, 2007 [cited from 2013].

Dijkmans PA, Juffermans LJ, Musters RJ, van Wamel A, ten Cate FJ, van Gilst W, Visser CA, de Jong N, Kamp O, Microbubbles and ultrasound: from diagnosis to therapy. Eur J Echocardiogr 2004; 5:245-56.

Ferrara K, Pollard R, Borden M, Ultrasound microbubble contrast agents: fundamentals and application to gene and drug delivery. Annu Rev Biomed Eng 2007; 9:415-47.

Guo Z, Hong S, Jin X, Luo Q, Wang Z, Wang Y, Study on the multidrug resistance 1 gene transfection efficiency using adenovirus vector enhanced by ultrasonic microbubbles in vitro. Mol Biotechnol 2011; 48:138-46.

Heath CH, Sorace A, Knowles J, Rosenthal E, Hoyt K, Microbubble therapy enhances anti-tumor properties of cisplatin and cetuximab in vitro and in vivo. Otolaryngol Head Neck Surg 2012; 146:938-45.

Kaplan JM, Adenovirus-based cancer gene therapy. Curr Gene Ther 2005; 5:595-605.

Kim KH, Dmitriev I, O'Malley JP, Wang M, Saddekni S, You Z, Preuss MA, Harris RD, Aurigemma R, Siegal GP, Zinn KR, Curiel DT, Alvarez RD, A phase I clinical trial of Ad5.SSTR/TK.RGD, a novel infectivity-enhanced bicistronic adenovirus, in patients with recurrent gynecologic cancer. Clin Cancer Res 2012; 18:3440-51.

Klibanov AL, Microbubble contrast agents: targeted ultrasound imaging and ultrasound-assisted drug-delivery applications. Invest Radiol 2006; 41:354-62.

Koike H, Tomita N, Azuma H, Taniyama Y, Yamasaki K, Kunugiza Y, Tachibana K, Ogihara T, Morishita R, An efficient gene transfer method mediated by ultrasound and microbubbles into the kidney. J Gene Med 2005; 7:108-16.

Lindner JR, Microbubbles in medical imaging: current applications and future directions. Nat Rev Drug Discov 2004; 3:527-32.

Lupold SE, Rodriguez R, Adenoviral gene therapy, radiation, and prostate cancer. Rev Urol 2005; 7:193-202.

McDannold N, Arvanitis CD, Vykhodtseva N, Livingstone MS, Temporary disruption of the blood-brain barrier by use of ultrasound and microbubbles: safety and efficacy evaluation in rhesus macaques. Cancer Res 2012; 72:3652-63.

Miller DL, Quddus J, Diagnostic ultrasound activation of contrast agent gas bodies induces capillary rupture in mice. Proc Natl Acad Sci USA 2000; 97:10179-84.

Nie F, Xu HX, Lu MD, Wang Y, Tang Q, Anti-angiogenic gene therapy for hepatocellular carcinoma mediated by microbubble-enhanced ultrasound exposure: an in vivo experimental study. J Drug Target 2008; 16:389-95.

Price RJ, Skyba DM, Kaul S, Skalak TC, Delivery of colloidal particles and red blood cells to tissue through microvessel ruptures created by targeted microbubble destruction with ultrasound. Circulation 1998; 98:1264-7.

Shimamura M, Sato N, Taniyama Y, Kurinami H, Tanaka H, Takami T, Ogihara T, Tohyama M, Kaneda Y, Morishita R, Gene transfer into adult rat spinal cord using naked plasmid DNA and ultrasound microbubbles. J Gene Med 2005; 7:1468-74.

Shohet RV, Chen S, Zhou YT, Wang Z, Meidell RS, Unger RH, Grayburn PA, Echocardiographic destruction of albumin microbubbles directs gene delivery to the myocardium. Circulation 2000; 101:2554-6.

Sirsi SR, Borden MA, Advances in ultrasound mediated gene therapy using microbubble contrast agents. Theranostics 2012; 2:1208-22.

Sirsi SR, Hernandez SL, Zielinski L, Blomback H, Koubaa A, Synder M, Homma S, Kandel JJ, Yamashiro DJ, Borden MA, Polyplex-microbubble hybrids for ultrasound-guided plasmid DNA delivery to solid tumors. J Control Release 2012; 157:224-34.

Song J, Chappell JC, Qi M, VanGieson EJ, Kaul S, Price RJ, Influence of injection site, microvascular pressure and ultrasound variables on microbubble-mediated delivery of microspheres to muscle. J Am Coll Cardiol 2002; 39:726-31.

Sorace AG, Saini R, Rosenthal E, Warram JM, Zinn KR, Hoyt K, Optical fluorescent imaging to monitor temporal effects of microbubble-mediated ultrasound therapy. IEEE Trans Ultrason Ferroelectr Freq Control 2013; 60:281-9.

Sorace AG, Warram JM, Umphrey H, Hoyt K, Microbubble-mediated ultrasonic techniques for improved chemotherapeutic delivery in cancer. J Drug Target 2012; 20:43-54.

Treat LH, McDannold N, Zhang Y, Vykhodtseva N, Hynynen K, Improved Anti-Tumor Effect of Liposomal Doxorubicin After Targeted Blood-Brain Barrier Disruption by MRI-Guided Focused Ultrasound in Rat Glioma. Ultrasound Med Biol 2012; 38:1716-25.

Tsunoda S, Mazda O, Oda Y, Iida Y, Akabame S, Kishida T, Shin-Ya M, Asada H, Gojo S, Imanishi J, Matsubara H, Yoshikawa T, Sonoporation using microbubble BR14 promotes pDNA/siRNA transduction to murine heart. Biochem Biophys Res Commun 2005; 336:118-27.

Wang JF, Wu CJ, Zhang CM, Qiu QY, Zheng M, Ultrasound-mediated microbubble destruction facilitates gene transfection in rat C6 glioma cells. Mol Biol Rep 2009; 36:1263-7.

Wang X, Liang HD, Dong B, Lu QL, Blomley MJ, Gene transfer with microbubble ultrasound and plasmid DNA into skeletal muscle of mice: comparison between commercially available microbubble contrast agents. Radiology 2005; 237:224-9.

Warram JM, Sorace AG, Saini R, Borovjagin AV, Hoyt K, Zinn KR, Systemic delivery of a breast cancer-detecting adenovirus using targeted microbubbles. Cancer Gene Ther 2012; 19:545-52.

Zhang Q, Wang Z, Ran H, Fu X, Li X, Zheng Y, Peng M, Chen M, Schutt CE, Enhanced gene delivery into skeletal muscles with ultrasound and microbubble techniques. Acad Radiol 2006; 13:363-7.

FIGURE LEGENDS

Figure 1. (a) Representative bioluminescence images of plated cancer cells incubated with Ad vectors after exposure to high pressure US-stimulated therapy or sham (control) US. Detailed analysis of the bioluminescent signal (counts) representing Ad infection efficiency after the Ad vector was exposed to acoustic conditions akin to that used during US-stimulated therapy (c). Sham or US exposure at low or high acoustic pressures did not produce any differential effects or alterations in Ad infectivity potential. The application of US-stimulated therapy to cancer cell cultures incubated with an Ad vector resulted in no singificant differences in bioluminescence images (b) or the Ad infectivity rate (d), which again indicates US had no negative effects on Ad vector infectivity or the transduction pathway.

Figure 2. (a) US-stimulated therapy improves delivery of the Ad vector to the target flank tumors especially at low Ad concentrations. (b) Representative bioluminescence images at baseline and 48 hours after US-stimulated therapy for various Ad concentrations denoted as low, moderate, and high. US-stimulated therapy produced an increase in bioluminescence signal measurements (via increased Ad infection) over contralateral control tumors at various Ad concentration levels (bottom).

Figure 3. Analysis of individual animals in the low Ad concentration group which demonstrated the greatest enhancement after receiving US-stimulated therapy. Of the animals investigated, 75% of the tumors produced increased bioluminescence signals compared to contralateral tumor measurements. These findings were attribued to improved Ad retention and infectivity in the target tumor receiving US-stimulated therapy.

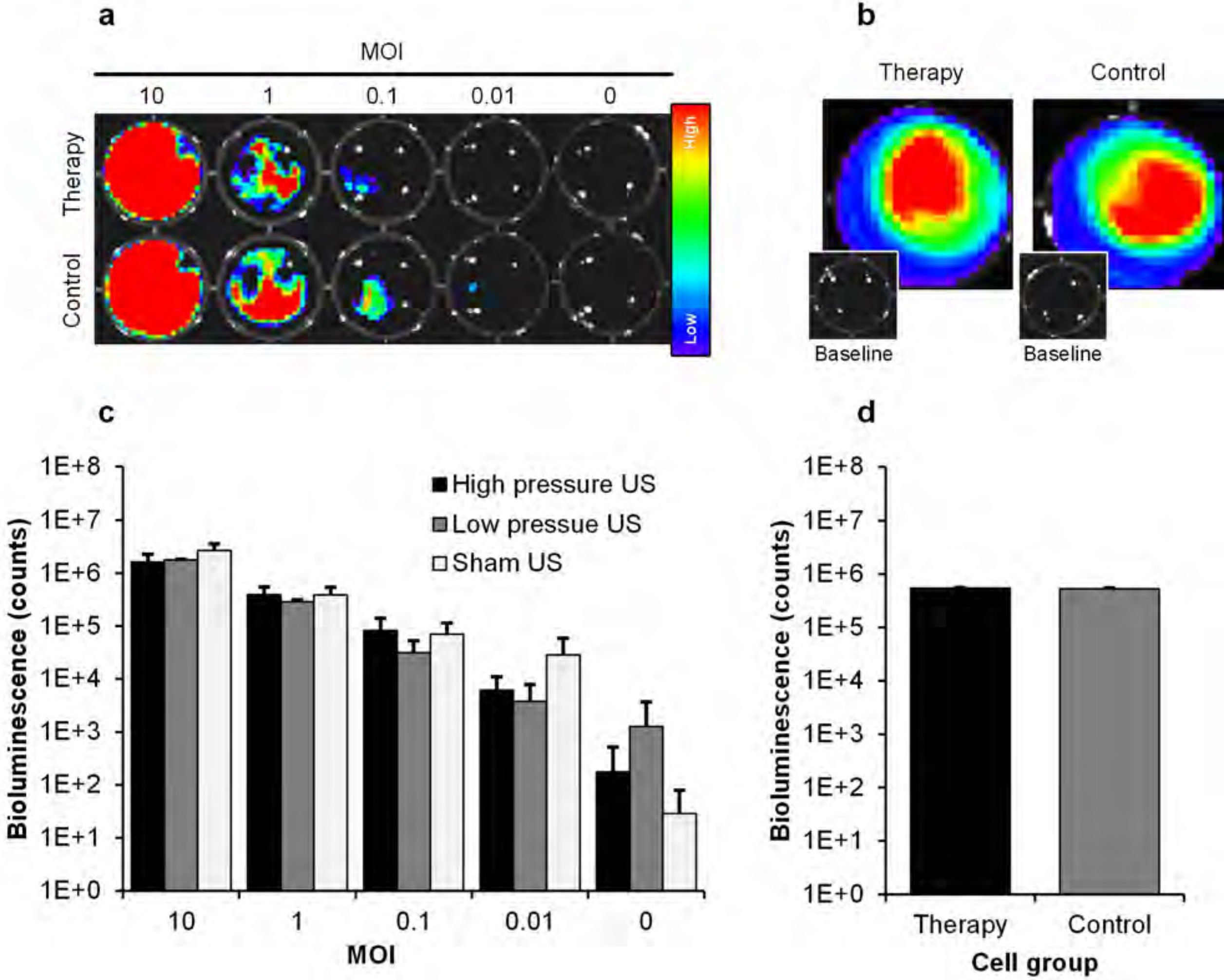
a
MOI
10
1
0.1
0.01
0
Therapy
Control
High
Low
b
Therapy
Control
Baseline
Baseline
c
1E+8
1E+7
1E+6
1E+5
1E+4
1E+3
1E+2
1E+1
1E+0
Bioluminescence (counts)
High pressure US
Low pressue US
Sham US
10
1
0.1
0.01
0
MOI
d
Bioluminescence (counts)
Therapy
Control
Cell group

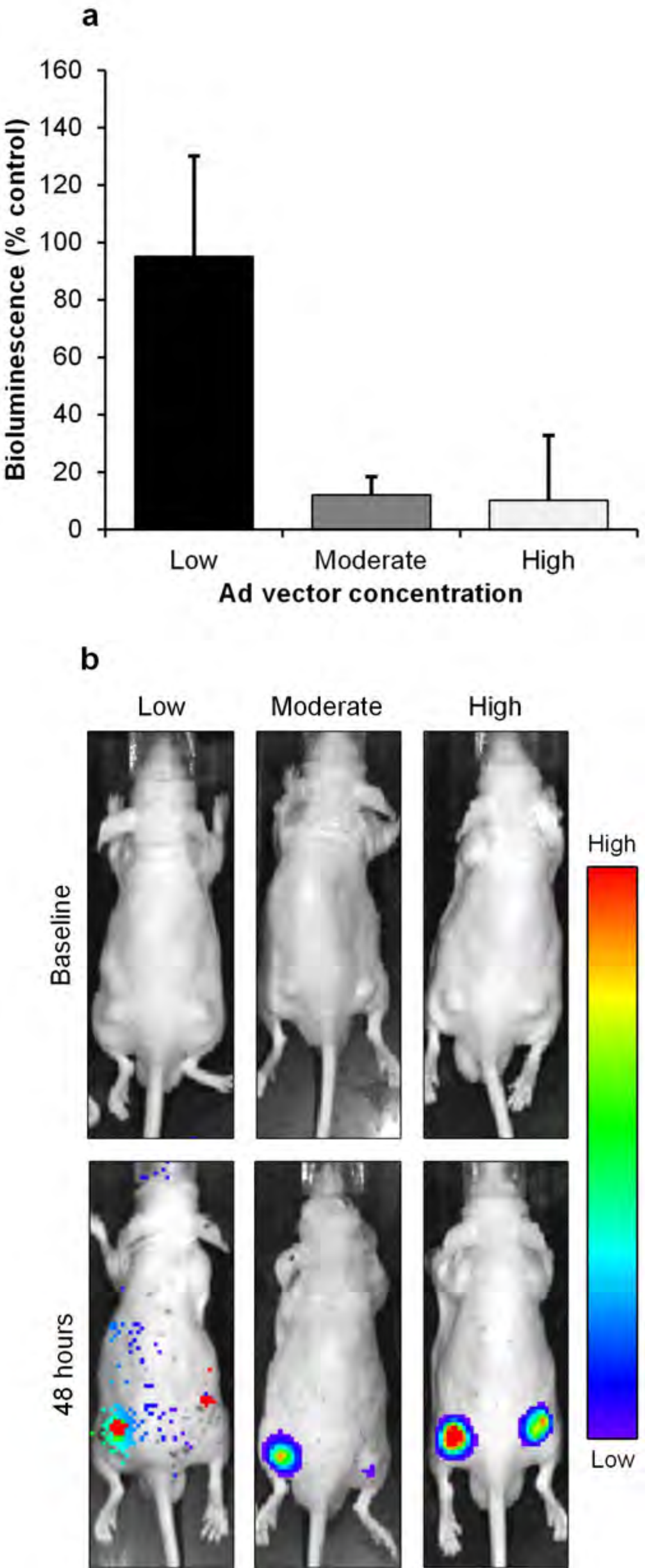

a
Bioluminescence (% control)
160
140
120
100
80
60
40
20
0
Low
Moderate
High
Ad vector concentration
b
Low
Moderate
High
Baseline
48 hours
High
Low

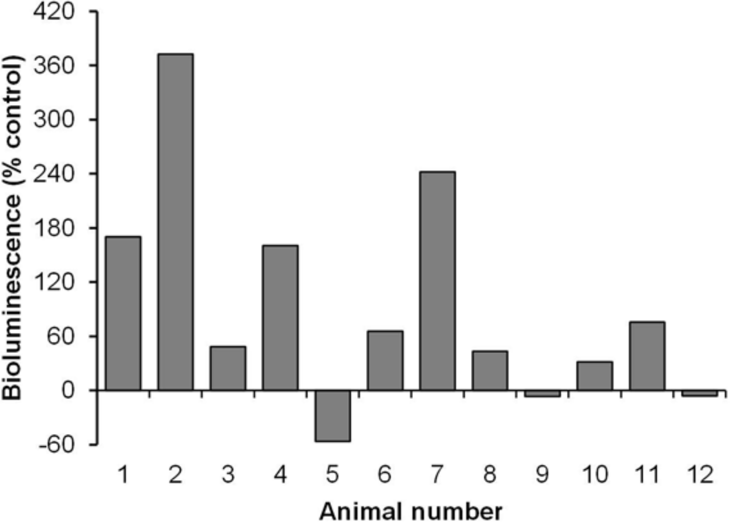

420
360
300
240
180
120
60
0
-60
Bioluminescence (% control)
1
2
3
4
5
6
7
8
9
10
11
12
Animal number